

Manuscript of the article: Gabriella Satori, Earle Williams, Colin Price, Robert Boldi, Alexander Koloskov, Yuri Yampolski, Anirban Guha, Veronika Barta, Effects of Energetic Solar Emissions on the Earth–Ionosphere Cavity of Schumann Resonances.

Appeared in: Surveys in Geophysics, July 2016, Volume 37, Issue 4, pp 757–789

DOI 10.1007/s10712-016-9369-z

The final publication is available at link.springer.com:

<http://link.springer.com/article/10.1007/s10712-016-9369-z>



2

3 Effects of Energetic Solar Emissions on the Earth– 4 Ionosphere Cavity of Schumann Resonances

5 Gabriella Sátori¹ · Earle Williams² · Colin Price³ ·
6 Robert Boldi⁴ · Alexander Koloskov⁵ · Yuri Yampolski⁵ ·
7 Anirban Guha⁶ · Veronika Barta¹

8 Received: 24 April 2015 / Accepted: 25 February 2016
9 © Springer Science+Business Media Dordrecht 2016

10 **AQ1 Abstract** Schumann resonances (SR) are the electromagnetic oscillations of the spherical
11 cavity bounded by the electrically conductive Earth and the conductive but dissipative
12 lower ionosphere (Schumann in Z Naturforsch A 7:6627–6628, 1952). Energetic emissions
13 from the Sun can exert a varied influence on the various parameters of the Earth’s SR:
14 modal frequencies, amplitudes and dissipation parameters. The SR response at multiple
15 receiving stations is considered for two extraordinary solar events from Solar Cycle 23: the
16 Bastille Day event (July 14, 2000) and the Halloween event (October/November 2003).
17 Distinct differences are noted in the ionospheric depths of penetration for X-radiation and
18 solar protons with correspondingly distinct signs of the frequency response. The prefer-
19 ential impact of the protons in the magnetically unshielded polar regions leads to a marked
20 anisotropic frequency response in the two magnetic field components. The general
21 immunity of SR amplitudes to these extreme external perturbations serves to remind that
22 the amplitude parameter is largely controlled by lightning activity with the Earth–iono-
23 sphere cavity.

24 **Keywords** Schumann resonances · Solar X-ray · Solar proton · Earth–ionosphere cavity ·
25 Characteristic ionospheric heights
26

A1 Gabriella Sátori
A2 gsatori@ggki.hu

A3 ¹ Research Centre for Astronomy and Earth Sciences, Hungarian Academy of Sciences, Geodetic
A4 and Geophysical Institute, Csatkai u. 6-8., Sopron, Hungary

A5 ² Parsons Laboratory, MIT, Cambridge, MA, USA

A6 ³ Tel Aviv University, Tel Aviv, Israel

A7 ⁴ Zayed University, Abu Dhabi, United Arab Emirates

A8 ⁵ Institute of Radio Astronomy, National Academy of Sciences of Ukraine, 4 Chernovopravorna St.,
A9 Kharkiv 61002, Ukraine

A10 ⁶ Tripura University, Suryamaninagar, India



27 1 Introduction

28 **AQ2** The Earth's naturally occurring Schumann resonances (SR), maintained by global lightning
29 and confined to the thin dielectric region of atmosphere between the conductive Earth
30 and the ionosphere, are rich with information about the terrestrial and space environments.
31 These continuously maintained global resonances are characterized by amplitudes (inten-
32 sities), modal frequencies and dissipation parameters (Q factors and damping param-
33 eters), all of which respond in distinct ways to different kinds of forcing. This study is
34 concerned with the impacts of exceptional solar activity on the parameters of the SR.

35 Two of the most exceptional solar storms on record that also serve to bracket the solar
36 maximum of Solar Cycle 23 have been selected for detailed examination, the Bastille Day
37 event of July 14, 2000 and the Halloween event of October/November, 2003. The Bastille
38 Day event, an X-class (5) solar flare with a distinct separation of X-radiation and solar
39 proton emissions, has already been identified as a choice target for both experimental ELF
40 studies (Nickolaenko and Hayakawa 2002; Roldugin et al. 2004; De et al. 2010; Nicko-
41 laenko and Hayakawa 2014) and modeling work (Ondráškova et al. 2003; Ondráškova
42 2005). The Halloween event, a solar disturbance of exceptionally long duration in spanning
43 a two-month period (Baker et al. 2004), saturated the hard X-ray detectors on the GOES
44 satellite (Lopez et al. 2004). Subsequent analysis led to an upgrade in the X-class of the last
45 flare of the sequence (November 4, 2003) to 45 (Thomson et al. 2004), making it the most
46 energetic solar flare on record. The effects of the Halloween event have not been previ-
47 ously examined at ELF, though a comparison of the solar emissions in the record-breaking
48 Bastille Day and Halloween events can be found in Le et al. (2007).

49 Key objectives in this investigation of SR response to these exceptional events have
50 been the establishment of a systematic global response and an exploration of evidence for a
51 timescale independence in the physical response, when the SR cavity is exposed to similar
52 levels of ionizing radiation but on very different timescales. An important reference for the
53 longer timescale is the response of SR to the 11-year solar cycle (Sátori et al. 2005). Also,
54 in light of the long-standing interest in using multi-station measurements of SR intensity as
55 a continuous monitor of global lightning activity (Williams and Mareev 2014), we have
56 been interested in the degree of immunity in the SR intensity to extraterrestrial influences
57 of the kind considered here.

58 The organization of this paper runs as follows. Section 2 is concerned with a description
59 of the five ELF stations worldwide that have provided SR documentation on the two
60 selected events. Section 3 reviews previous work on this subject, including the discussion
61 of the ionization profiles for mono-energetic particles that are so useful in relationship with
62 the ‘electric’ (h_e) and magnetic (h_m) ionospheric heights for SR. In Sect. 4, the results on
63 measured SR response in frequency and intensity (field amplitude squared) are presented.
64 The results are discussed in comparison with the theoretical predictions in Sect. 5, fol-
65 lowed by the conclusions in the final Sect. 6.

66 2 Observational Assets

67 The interest in this study in establishing a global response to energetic particles and
68 photons from the Sun during extraordinary events led to the examination of Schumann
69 resonance observations at widely separated ELF receiving stations. Data from five separate
70 observatories have been used, as summarized in Table 1. Four of these stations are



Table 1 Location and SR parameters of five separate SR stations

Location	Lat	Long	Field component	Mode number
Mitzpe Ramon, Israel	30.6 N	34.8 E	E_Z , H_{EW} , H_{NS}	1st, 2nd, 3rd
Nagyencenk, Hungary	46.7 N	16.7 E	E_Z	1st, 2nd, 3rd
Parkfield, California, USA	35.9 N	120.4 W	H_{EW} , H_{NS}	1st
Vernadsky, Antarctica, Ukraine	65.3 S	64.2 W	H_{EW} , H_{NS}	1st, 2nd, 3rd
West Greenwich, Rhode Island, USA	41.6 N	71.7 W	E_Z , H_{EW} , H_{NS}	1st, 2nd, 3rd

71 operated continuously by co-authors of this paper and include Nagycenk Observatory in
72 Hungary, Mitzpe Ramon Observatory in Israel, the MIT field station in West Greenwich,
73 Rhode Island and the Vernadsky, Antarctica station operated by the Ukraine. Additional
74 observations for Parkfield, California, established as part of an earlier earthquake moni-
75 toring effort there, were obtained from the Web site of the Berkeley Seismological Lab-
76 oratory (<http://www.quake.geo.berkeley.edu>).

77 It is important to note that Schumann resonance modal frequencies were estimated with
78 different methods in this study, with nearly as many variants as there are observatories
79 involved. For the Nagycenk observations, the complex demodulation method (Sátori et al.
80 1996; Verő et al. 2000) was used. For Parkfield data, the Prony algorithm was used (Füllekrug
81 1994). For Mitzpe Ramon and Rhode Island, conventional three-parameter Lorentzian fits
82 (Mushtak and Williams 2002; Sátori et al. 2009) were applied to extract frequencies. Finally,
83 for Vernadsky data, yet a different method was used for modal frequency estimation, and in
84 the absence of published documentation, that will be reviewed briefly here:

85 Power spectra S_{ew} and S_{ns} are computed for the east–west and north–south components
86 of magnetic field, respectively, and are computed at 10-min intervals. The weighted mean
87 modal frequency for the i th mode, fpi , of the respective magnetic field, is then computed as
88 follows:

$$fpi_{ns,ew} = \frac{\int_{fp0i-\Delta f}^{fp0i+\Delta f} df \cdot S_{ns,ew}(f) \cdot f}{\int_{fp0i-\Delta f}^{fp0i+\Delta f} df \cdot S_{ns,ew}(f)}$$

90 For first SR mode for example, values used for the integration limits are $fp01 = 8$ Hz
92 and $\Delta f = 1.5$ Hz.

93 For later quantitative comparisons with theoretical predictions, use will be made of the
94 SR modal frequencies from Rhode Island and Israel based on Lorentzian fits. All such fits
95 are applied to computed power spectra and so the Lorentzian fits to those spectra represent
96 intensity, not amplitude.

97 It is also important to note that the modal frequencies are not exactly equal to the eigen-
98 modal frequencies. The latter quantities are invariants of the cavity and should be measured
99 by every observer everywhere. The modal frequencies also depend on the source (S) to
100 observer (O) distance in the lossy Earth–ionosphere cavity (Balser and Wagner 1962;
101 Madden and Thompson 1965; Nickolaenko 1997; Nickolaenko and Hayakawa 2002). Kulak
102 et al. (2006) developed a decomposition method to separate the eigenmodal frequency from
103 the distance-dependent variations. This method was successfully applied for a sudden



104 ionospheric disturbance at a single station by Dyrda et al. (2015), and more recently for two
105 stations, one in Poland and the other in the USA (Kulak and Dyrda, personal communication
106 2016). The decomposition method claimed by Kulak et al. (2006) to separate the standing
107 (resonant) and traveling wave components cannot be applied to the events studied here
108 because the original time series data are not available for the five receiving stations involved.

109 3 Review of Previous Work

110 3.1 Impact of Energetic Particles on Upper and Lower D-Region Ionization

111 Energetic particles (electrons and protons primarily) and radiation (X-rays primarily),
112 emanating from the Sun and from space and impinging on the Earth's atmosphere have
113 characteristic depths of penetration as a function of energy. This aspect is particularly
114 important for the problem at hand because well-defined ionospheric heights are deemed
115 important for the behavior of SR (Madden and Thompson 1965; Greifinger and Greifinger
116 1978; Sentman 1990; Schlegel and Füllekrug 1999; Mushtak and Williams 2002;
117 Greifinger et al. 2007). Two special heights were first identified in research on SR (Madden
118 and Thompson 1965) when Maxwell's equations were applied to the Earth-ionosphere
119 waveguide cavity. The role of these heights has become so important since that time that
120 current models for the Schumann cavity are defined entirely with four complex heights,
121 two for daytime and two for nighttime ionospheres (Greifinger et al. 2007; Kulak and
122 Mlynarczyk 2013). The real part of the complex height is that physical height and the
123 imaginary part represents the scale height of that feature, with the scale heights generally
124 small in comparison with the physical heights. The effect of energetic particles on the
125 entire cavity then reduces simply to how these complex heights are affected by the
126 energetic particles (mainly photons, protons and electrons) and that is the main analysis
127 approach in the present work. The energy dependence of penetration depth has been
128 studied extensively for protons (Reid 1986), for electrons (Rees 1989) and for X-radiation
129 (Richmond and Venkateswaran 1971; Rees 1989; Hargreaves 1992), but this large body of
130 knowledge has not been strongly incorporated in previous studies of Schumann resonance
131 response to these effects. The increasing ionization with depth due to increases in air
132 density is accompanied by an attenuated flux with depth (dependent on the cross sections
133 for ionization by air molecules at the energies of interest), leaving well-defined 'Chapman
134 layers' of maximum ionization as a function of energy. The predictions for protons (Reid
135 1986) and electrons (Rees 1989) are reproduced in Fig. 1, with the assumption of no
136 magnetic shielding. Since proton energies exceeding 100 MeV are known to occur in
137 energetic solar events, penetration downward to ~30 km altitude is possible (Ondráškova
138 2005) in the unshielded high-latitude regions, with attendant effects on the lower char-
139 acteristic height of SR. It is important to note the additional evidence in Fig. 1 that when
140 proton energies are sufficient (>100 MeV) for maximum effect at 30 km, the ionization
141 impact in the upper characteristic layer is reduced by 2–3 orders of magnitude, and so is of
142 relatively negligible importance, even though the same protons pass through the upper
143 layer on their way down. On account of the substantially greater cross sections for air
144 ionization by protons than electrons, proton energies needed to reach the 80–90 km altitude
145 level (2–3 MeV) are substantially larger than for electrons (~50 keV). The X-radiation
146 considered in this study (0.1–0.8 nm in wavelength or 1.5–12 keV in energy) has still
147 smaller cross section for ionization and so still smaller photon energy is needed to attain
148 the same altitude. X-ray ionization profiles are not shown, but suffice it to say that the

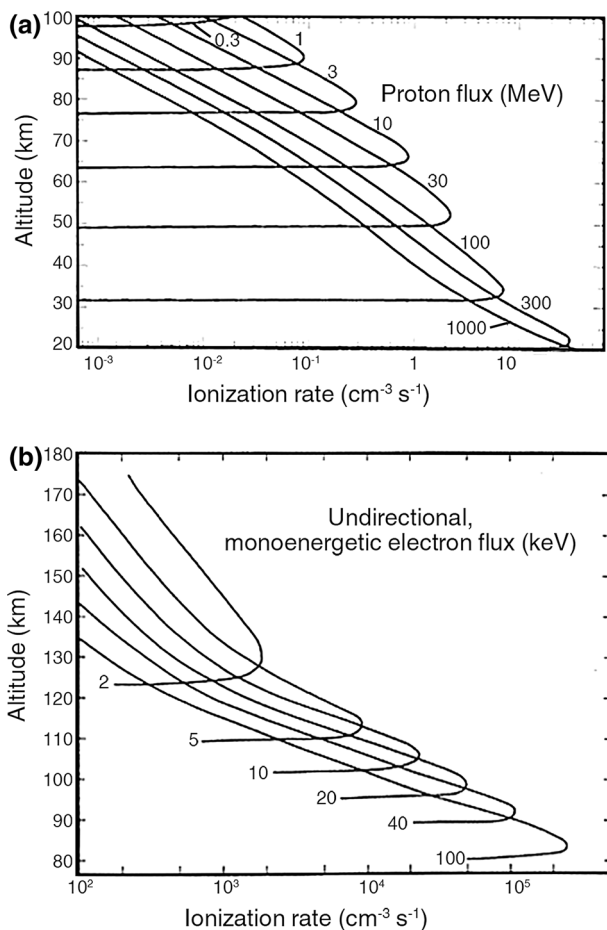


Fig. 1 Vertical profiles of ionization rate associated with the vertical entry of (a) mono-energetic protons adapted from Reid (1986) and (b) mono-energetic electrons adapted from Rees (1989) into the Earth's atmosphere. Magnetic shielding is assumed to be zero in both cases

149 ionization is maximum at 90 km altitude for X-rays in the wavelength range 0.2–1 nm
150 (Whitten and Popoff 1971; Brasseur and Solomon 1986; Hargreaves 1999).

151 3.2 Modifications of Schumann Resonances by Energetic Solar Emission

152 Important early work on the problem of energetic particle modification of the Earth–
153 ionosphere cavity has appeared, pertaining to both short-term (hours and days) and long-
154 term variations (11-year solar cycle).

155 3.2.1 Short Timescale

156 The early modeling work of Madden and Thompson (1965) set the stage for understanding
157 cavity response to ionizing radiation on short timescales by first identifying two key



158 dissipation heights in the D-region. The pioneering work of Nelson (1967) in investigating
159 SR parameter variations (modal frequency and Q factor) linked with polar cap absorption
160 (PCA) events (involving solar protons) was built on Madden and Thompson (1965), but
161 has not been cited frequently in the literature on this topic because this doctoral thesis was
162 never published. Nelson (1967) investigated three PCA events and found consistent results
163 in all cases: systematic decreases in SR frequency and Q factor for the fundamental 8 Hz
164 mode. Nelson (1967) recognized on the basis of his modeling work that ionization
165 increases in the lower characteristic height could account for the observed decreased
166 quantities, but also that ionization increases in the upper characteristic layer (now recog-
167 nized to be enacted by less deeply penetrating solar X-radiation) would lead to increases in
168 frequency and Q factor. Sorting out the contributions of competing effects from energetic
169 protons and photons (X-rays) has become an important goal in the present study.

170 Independently of Madden and Thompson (1965), and without awareness of the latter
171 work, Greifinger and Greifinger (1978) developed analytic predictions for the two char-
172 acteristic heights. [The analytical form of the lower height matched that of Madden and
173 Thompson (1965)]. Due to the convenience of the analytical form, much of the subsequent
174 work on mono-energetic particle modification of the Earth-ionosphere cavity (Schlegel
175 and Füllekrug 1999; Sátori et al. 2005; Shvets et al. 2005) has relied on the Greifinger
176 approach.

177 Roldugin et al. (1999) first identified the distinct contributions of energetic protons and
178 X-radiation to Schumann resonance frequency perturbations in relativistic solar proton
179 precipitation on November 6, 1997. Later, the same authors documented a similar sequence
180 of X-rays followed by energetic protons in the extraordinary Bastille Day event of 2000,
181 and again with distinct SR frequency variations made possible by the non-overlapping of
182 these two fluxes in time during the event. The evidence for the different preferential
183 ionization heights for protons (with energies in the 1–100 MeV range) and for solar
184 X-radiation (with energies in the range of 10–30 keV) had been discussed qualitatively by
185 Sentman (1990), but was specified more quantitatively in Reid (1986) for protons and by
186 Richmond and Venkateswaran (1971), Rees (1989) and Hargraves (1992) for the X-ra-
187 diation as discussed above. Ondráškova's (2005) model calculations for the Bastille Day
188 event provide important evidence that the solar protons can strongly influence the lower
189 characteristic height of SR while exerting only minor influence on the upper height.
190 Roldugin's documentation of systematic increases in SR frequency in response to X-ray
191 events (including the analysis on the Bastille Day event), and the findings of a pronounced
192 global response to X-rays on the solar cycle timescale (Sátori et al. 2005), both call into
193 question claims that the effects of X-radiation on the Schumann cavity are negligible
194 (Nickolaenko and Hayakawa 2002). Roldugin's pioneering work underlines the need for
195 fine time resolution (10 min or better) in both the solar emissions and the global frequency
196 variations.

197 On rare occasion, the Earth's atmosphere is subjected to photon bombardments from the
198 cosmos with energies (tens of MeV, Palmer et al. 2005) one thousand times greater than
199 that of solar X-radiation. One such gamma ray event on August 27, 1998, studied by Price
200 and Mushtak (2001) showed "no noticeable changes in the ELF signals". This negative
201 result may have explanation in the fact that the main ionization altitude from such ener-
202 getic events does not coincide with either of two characteristic heights of the SR cavity
203 (Greifinger et al. 2007). The gamma flare on December 27, 2004, studied later (Tanaka
204 et al. 2011; Nickolaenko et al. 2012) also showed no discernible effect on SR propagation
205 parameters, as in Price and Mushtak (2001), but it did produce a conspicuous ELF pulse.



206 Chapman and Jones (1964), Schlegel and Füllekrug (1999) and Shvets et al. (2005) have
207 all noted frequency increases associated with solar proton events. Madden and Thompson
208 (1965) registered surprise with the finding of Chapman and Jones (1964) but at that time
209 the documentation of accompanying X-radiation was rather incomplete. Shvets et al.
210 (2005) dubbed these events “anti-PCA events”. Their interpretation of these events
211 involved a decrease of the upper characteristic height, but with no role for X-rays. The
212 common presence of both proton and X-ray emission in solar flares is now well estab-
213 lished. The SR frequency observations of Schlegel and Füllekrug (1999) were limited to
214 daily resolution, and so the changes in frequency from the X-ray-dominant to the solar
215 proton-dominant portion of events they studied [e.g., October 1989, shown in detail for
216 both protons and X-rays in Belov et al. (2005)] could not be examined.

217 The polar non-uniformity of solar proton events in the Schumann resonance context has
218 been appropriately emphasized by Rabinowicz et al. (2008). The key role of the Earth’s
219 dipolar magnetic field in guiding energetic protons and electrons into polar regions must be
220 considered in interpreting results with a uniform model.

221 3.2.2 Long Timescale

222 The variation in D-region ionization by solar X-radiation and protons over the 11-year
223 solar cycle has also been manifest in numerous observations of the SR (Sátori et al. 2000;
224 Füllekrug et al. 2002; Kulak et al. 2003; Sátori et al. 2005; Ondráškova et al. 2011).
225 Figure 16 serves as a reminder about the two-order-of-magnitude variation in X-ray flux
226 from the Sun over the solar cycle. The strong spikes associated with individual X-ray
227 events are superimposed on a continuously varying background level of X-radiation
228 (Veronig et al. 2004). The 11-year variation of solar protons in the energy range >10 MeV
229 consists of two-order-of-magnitude variations in average fluence from individual solar
230 proton events (Feynman et al. 1990), but such high-energy events are sporadic in time and
231 often disappear for months on end during solar minima (Getselev et al. 2006). The mag-
232 netic intensity variations at Vernadsky (Antarctica) suggest a substantial solar cycle
233 variation (Williams et al. 2014). Based on discussions (D. Baker, B. Blake, H. Spence,
234 personal communication December 2014), we now suspect that energetic electrons from
235 the inner radiation belt are primarily responsible for the modification of the Schumann
236 cavity on the solar cycle timescale at high latitudes.

237 4 Results on Two Extraordinary Solar Events

238 Two exceptional solar events have been selected for multiple-station Schumann resonance
239 analysis in this study with two main goals in mind. The first is to establish the global
240 representativeness of the Schumann signatures, and single-station analyses of the Bastille
241 Day event (Nickolaenko and Hayakawa 2002; Roldugin et al. 2004; De et al. 2010) are
242 available for comparison with the new observations reported here. The second goal is to
243 document the Schumann resonance response to X-rays and protons on a distinctly different
244 timescale than is typical for the Bastille Day kind of event on the short timescale, and for
245 the 11-year solar cycle response on the long timescale.



246 4.1 The Bastille Day Event

247 4.1.1 Frequency Variations

248 This giant solar proton event occurred on July 14, 2000. This event is known in the
249 literature as the Bastille Day Event and the chronology of the solar emissions has been
250 studied by Bieber et al. (2002). It was preceded by a short but intense X-ray burst in the
251 X-class, the highest possible designation. (Of all solar events occurring since this time,
252 only the soon-to-be discussed Halloween Event exceeded this level in the X-radiation.)
253 Figure 2 shows the SR frequency variations for three resonant modes and for three field
254 AQ4 components at West Greenwich, Rhode Island. Remarkably similar to the records for the
255 same event shown in single-field components by Roldugin et al. (2004) in Kamchatka, and
256 by De et al. (2010) in India, with the signs of the frequency changes well-timed and with
257 well-separated arrivals for X-rays and protons at the Earth's ionosphere in all cases. (This
258 separation in time (~ 90 min) greatly simplifies the interpretation of the observations for
259 the Bastille Day event in comparison with the situation for the Halloween event to be

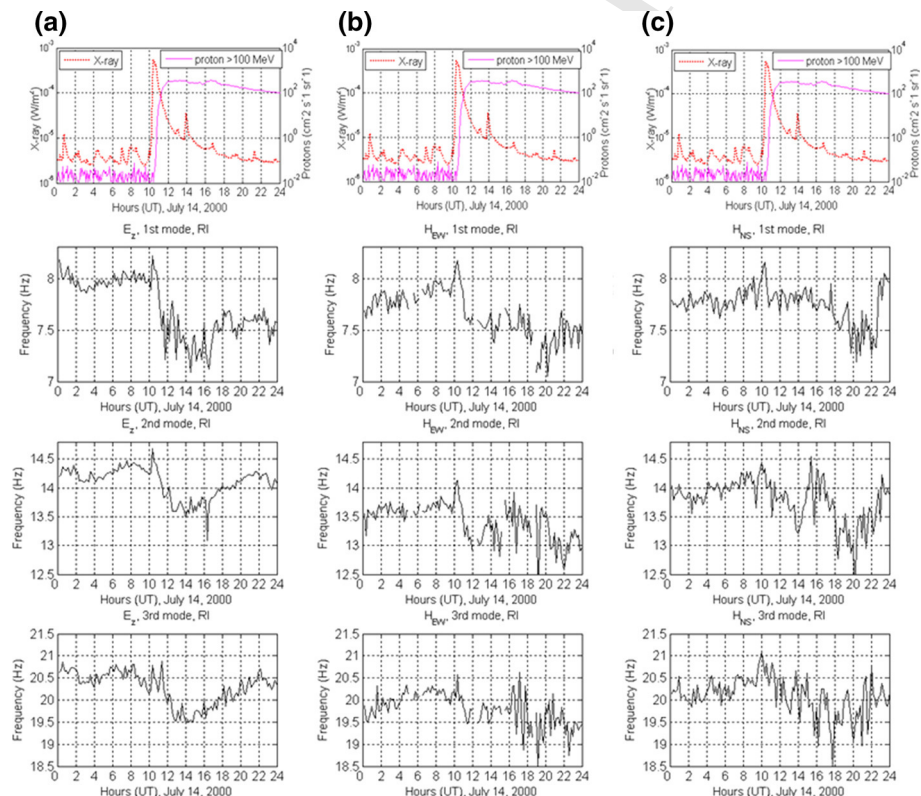


Fig. 2 Simultaneous records of the Schumann resonance frequency variations in West Greenwich, Rhode Island (in Hertz) during the Bastille Day Event (July 14, 2000) for (a) the vertical component of the electric field, for three resonance modes (left hand column), for (b) the H_{BW} component of the magnetic field, for three resonance modes (middle column) and for (c) the H_{NS} component of the magnetic field, for three resonance modes. The repeated records at the top of each column show the simultaneous history of the X-rays (first arrival) followed by the solar protons



discussed.) All modal frequencies increased during the short duration X-ray burst (at 10:24 UT) and then decreased markedly for several hours (11–16 UT) in all components of electric and magnetic field components in Rhode Island (see Fig. 2). The frequency increases evident in Fig. 2 and quantified in Table 4 of the “Appendix” were determined between the time of the maximum X-ray flux and the 3-h mean frequency value preceding it. The huge frequency decreases were estimated between the time of the maximum flux of the X-ray burst (10:24 UT) and the mean frequency level measured during the 3 h of maximum flux of the solar proton event.

268 4.1.2 The Bastille Day Event Results on Intensity Variations

269 Given the expectation for the deformation of the Schumann resonance cavity by these
270 exceptionally energetic extraterrestrial ionizing events, it is of interest to explore the
271 possibility of variations in the intensity of the SR simultaneous with that deformation.
272 Figure 3 shows the intensity variations for the first resonance mode in West Greenwich,
273 Rhode Island, for 4 days surrounding the Bastille Day event, together with the record of
274 the proton flux ($E > 100$ MeV). The proton flux increased by about four orders of mag-
275 nitude between 10:00 UT and 10:30 UT on July 14, 2000 (<http://spidr.ngdc.noaa.gov/>)

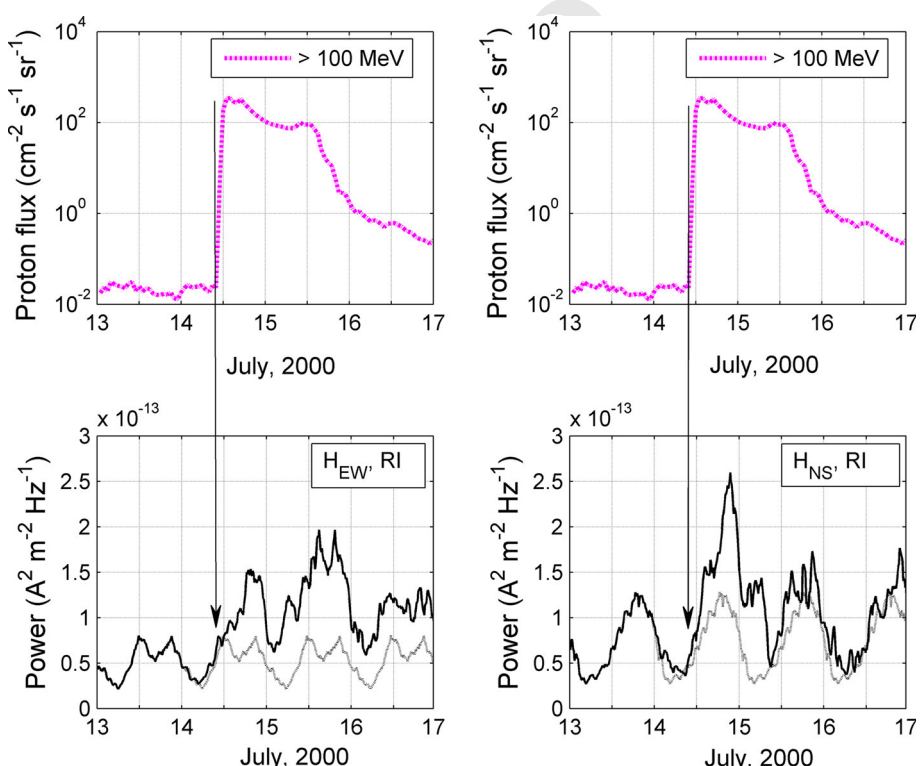


Fig. 3 Simultaneous records of the Schumann resonance intensity variations (in $\text{A}^2/\text{m}^2/\text{Hz}$) during 4 days surrounding the Bastille Day event (July 14, 2000) at West Greenwich, Rhode Island, with the H_{ew} field intensity variation on the *left* and the H_{ns} variation on the *right*. The intensity variation for July 13 is considered as a reference day and is repeated four times (*dashed curves*). The two (repeated) records at the *top* show the simultaneous history of energetic proton forcing

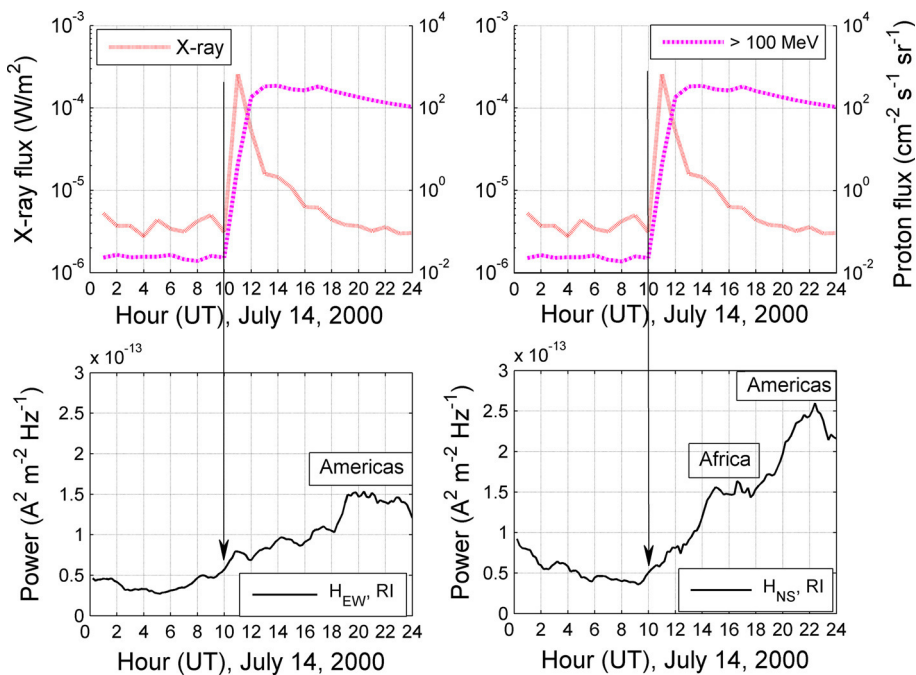


Fig. 4 Simultaneous records of the Schumann resonance intensity variations (in $\text{A}^2/\text{m}^2/\text{Hz}$) for the single day of the Bastille Day event (July 14, 2000) at West Greenwich, Rhode Island, for the H_{EW} component (middle) and the H_{NS} component (bottom). The simultaneous history of forcing by X-radiation and protons is repeated at the top

276 spidr/. The arrows in Figs. 3 and 4 indicate the time point 10:00 UT. At first glance, the
277 enhanced intensity (on the order of several tens of percent) noted on the day of the event
278 and the day following are strongly suggestive of a positive influence, but on closer
279 inspection at the time of the strong onset of the proton flux, no appreciable response in
280 intensity is noted. Since the timing of both data sets is accurately known, and since one has
281 every expectation that the effects of the ionizing radiation on the SR cavity are instantan-
282 eous, this latter observation casts some doubt on an appreciable effect of the protons on
283 SR intensity. One can take this analysis one step further by examining only the single day
284 of the event, in Fig. 4. For a summer day in Rhode Island, the diurnal records of H_{EW} and
285 H_{NS} are unusually free of local meteorological contamination, and one can see the presence
286 of the African and American sources in the two records. But the intensity response to the
287 energetic proton event is not remarkable in either record of magnetic field.

288 4.2 The Halloween Event

289 4.2.1 Frequency Variations

290 Figure 5 documents a series of dramatic emissions from the Sun over a period of several
291 weeks in October and November of 2003 (Baker et al. 2004) that has come to define the so-
292 called Halloween Event. The hard solar X-ray flux (0.1–0.8 nm) increased by more than
293 two orders of magnitude for a period longer than 2 weeks between October 18 and
294 November 4. The X-radiation from this unusual event (Lopez et al. 2004; Thomson et al.

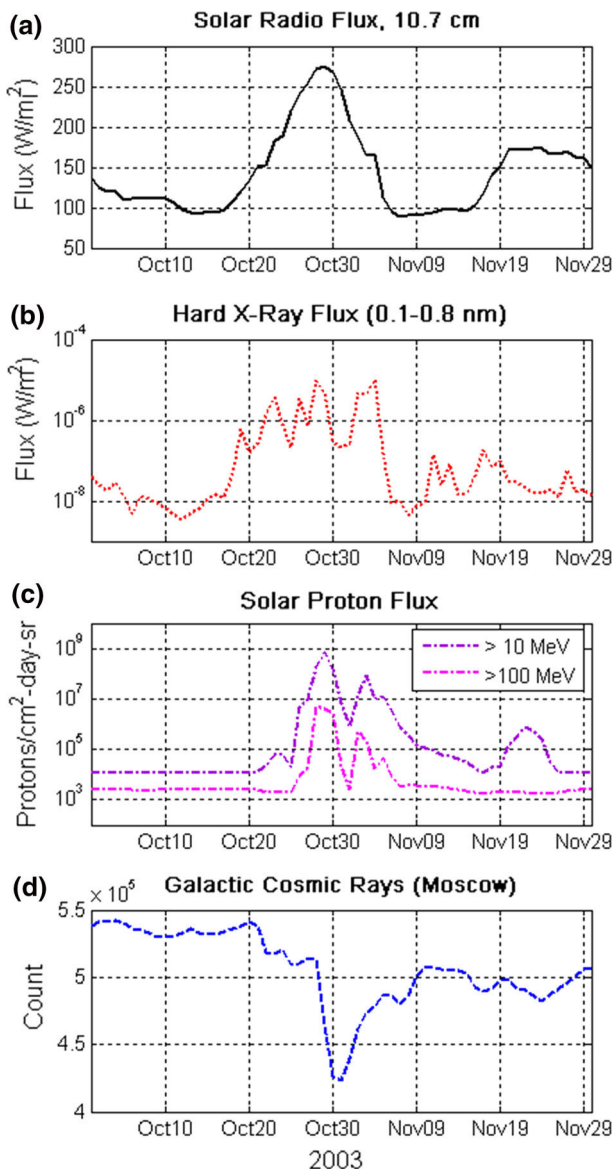


Fig. 5 Time histories of key quantities for the Halloween event of October/November 2003, including (a) the 10.7 cm microwave flux, (b) the GOES solar X-radiation flux (0.1–0.8 nm wavelength), (c) the GOES solar proton flux (in two energy ranges, >10 MeV and >100 MeV), and (d) the galactic cosmic ray count (recorded in Moscow). The timing of the maxima in fluxes of X-radiation and solar protons are generally consistent with specific solar events (flares and coronal mass ejections) documented in Lopez et al. (2004)

295 2004) is unprecedented in the era of GOES satellite measurements of hard X-rays. (The
296 GOES sensors were saturated on November 3 during an X-28 class solar flare, and the
297 analysis of that saturation lead to an upgrade in the classification to X-45.) The mean x-ray

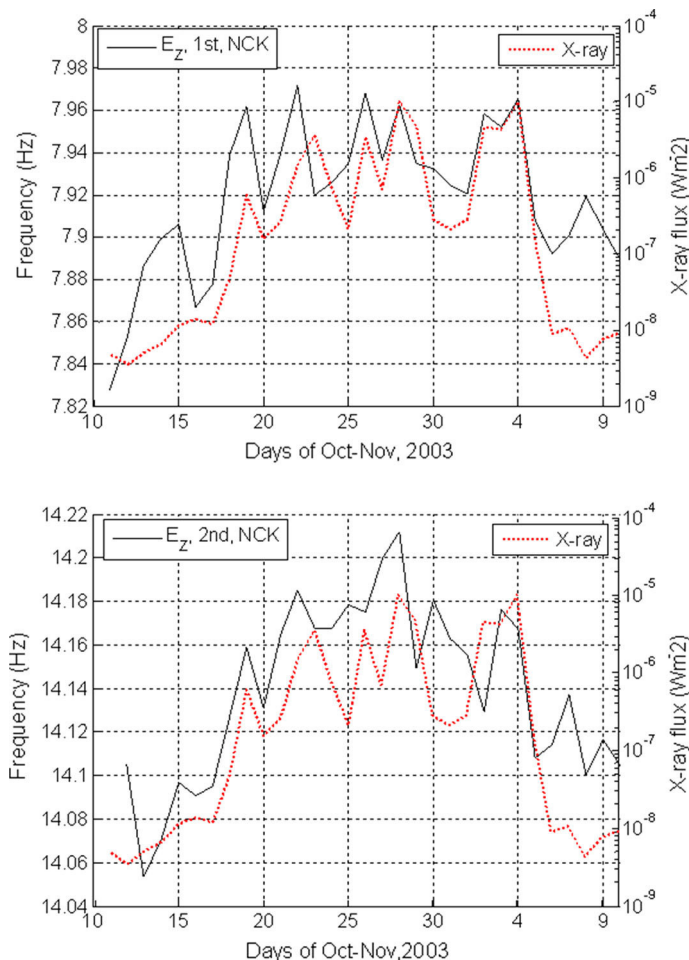


Fig. 6 Simultaneous records of Schumann resonance frequency variations (in Hertz) during the Halloween Event (October/November, 2003) in the first (top plot) and second (bottom plot) mode of the vertical electric field at Nagycenk (Hungary) Observatory, and the GOES solar X-radiation flux (0.1–0.8 nm wavelength). Note positive correlation of frequency variations and X-ray flux over the substructure of the X-ray record

298 flux was $2.7 \times 10^{-6} \text{ W/m}^2$ in this period in contrast with the mean level of $1 \times 10^{-8} \text{ W/m}^2$ in the 3 days before and after this strongly disturbed interval. All modal frequencies at 299 all SR stations increased during the days of increased X-ray flux for both the electric and 300 magnetic field components. This organized global behavior is shown by consistent 301 Schumann resonance frequency records at Nagycenk, Hungary (Fig. 6), Mitzpe Ramon, 302 Israel (Fig. 7), Parkfield, California (Fig. 9) and Vernadsky, Antarctica (Fig. 10) that are 303 all well correlated with the GOES satellite measured X-radiation. The magnitudes of the 304 frequency variations, extracted from these various time series records, are summarized in 305 Tables 5, 6, 7 and 8 in the “Appendix”. The frequency changes were estimated in the 306 same way as for the perturbed and reference levels for the X-ray flux variations. Within 307 this extended Halloween event, a giant solar proton event also occurred on October 25, 308



309 7 days after the onset of the marked X-ray activity. The increase of solar proton flux
310 (>10 MeV) was more than four orders of magnitude (10^{-1} – 10^3 protons/ $\text{cm}^{-2} \text{s}^{-1} \text{sr}^{-1}$)
311 with the maximum value on October 29. The period of increased frequencies was inter-
312 rupted in the case of the H_{EW} field component for each mode at the Mitzpe Ramon station
313 for some days near the time of peak values of solar proton flux, as shown in Fig. 8 and a
314 sudden decrease in frequency occurred on October 26 and for more than five consecutive
315 days when the solar proton flux still varied by more than two orders of magnitude. Then,
316 the frequencies began to increase again during the bursty X-ray period that persisted until
317 November 4. In this case, the frequency values measured on October 26 and the mean
318 frequency value of October 28–30 are compared as shown for H_{EW} at Mitzpe Ramon in
319 Table 5.

320 A regression analysis of the frequencies was performed using different combinations of
321 stations, field components, and modes for exactly the same time windows presented in
322 Figs. 6, 7, 8, 9 and 10. Although the time history of the event is lost in the regression
323 analysis, it can be seen in Figs. 11 and 12 that all combinations of frequency values exhibit
324 increasing trends. The increasing trend is especially important in case of the regression
325 analysis for PKD (Northern Hemisphere station) and VND (Southern Hemisphere station)
326 (see the subplots: Fig. 12a, b). This result excludes the possibility of a systematic
327 meridional source motion with respect to these two stations during the event as the 1st
328 magnetic mode is an excellent indicator of the source motion, too (Nickolaenko and
329 Hayakawa 2002). In the latter case, the regression analysis should have shown a decreasing
330 trend. (The frequency of the H_{EW} field component at PKD should be increasing when the
331 source moves away from the observer and simultaneously decreasing at VND when the
332 source approaches it and vice versa). The increasing trend of frequencies for the H_{NS} field
333 component at MR and PKD (see Fig. 11d) also excludes a systematic westward/eastward
334 motion of the sources from day to day during the observed period. The common increasing

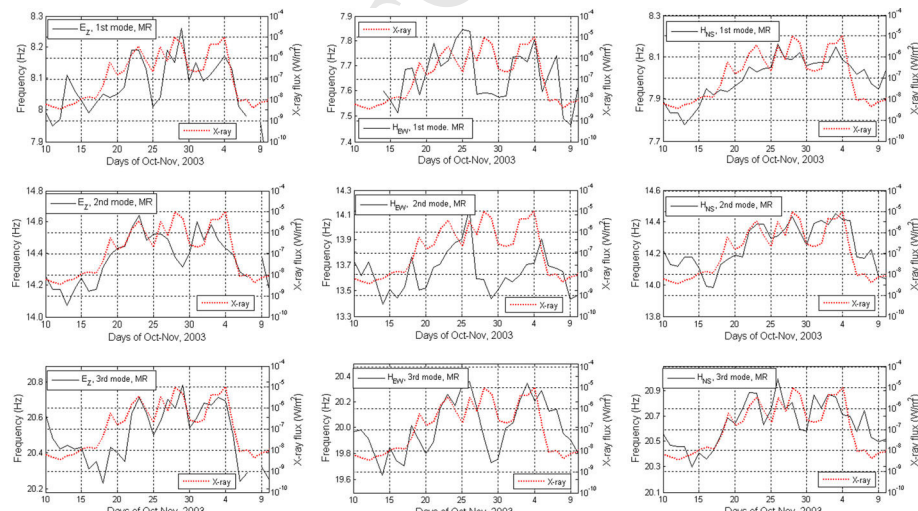


Fig. 7 Simultaneous records of Schumann resonance frequency variations (in Hertz) during the Halloween Event (October/November, 2003) for three field components (E_z , H_{EW} and H_{NS} , running left to right) and for three modes (running from top to bottom) at Mitzpe Ramon, Israel, and the GOES solar X-radiation flux (0.1–0.8 nm) (red, dashed, and repeated panel to panel)

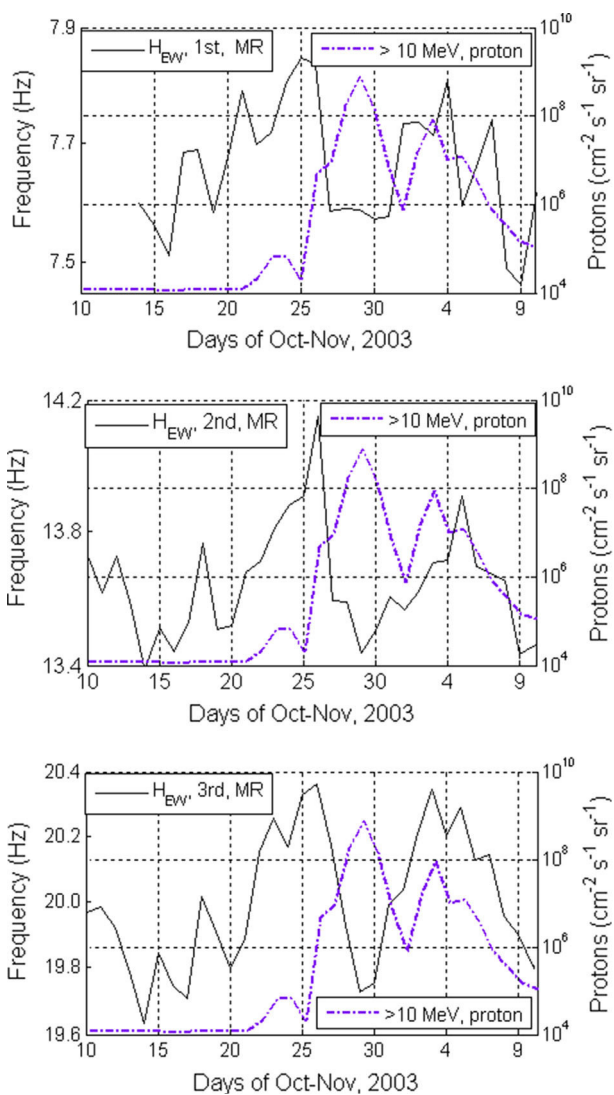


Fig. 8 Simultaneous records of Schumann resonance frequency variations (in Hertz) during the Halloween Event (October/November, 2003) for the H_{EW} component of magnetic field for three resonance modes (from top to bottom) at Mitzpe Ramon, Israel, and the GOES solar proton flux (>10 MeV) superimposed on each subplot (dashed, purple, and repeated panel to panel)

335 trends indicate the ionospheric origin of the frequency variations due to the excess ionization in the upper D-region attributed to the increased background solar X-ray flux by
336 more than two orders of magnitudes during the Halloween event (~ 2 weeks). Insignificant
337 trends were found only in those cases (subplots Figs. 11c, 12c) when the H_{EW} field
338 component recorded in MR was involved in the regression analysis. The increased fre-
339 quencies due to the increased X-ray flux were interrupted by a large decrease of frequency
340 during the huge solar proton event discussed as the manifestation of an anisotropic wave
341

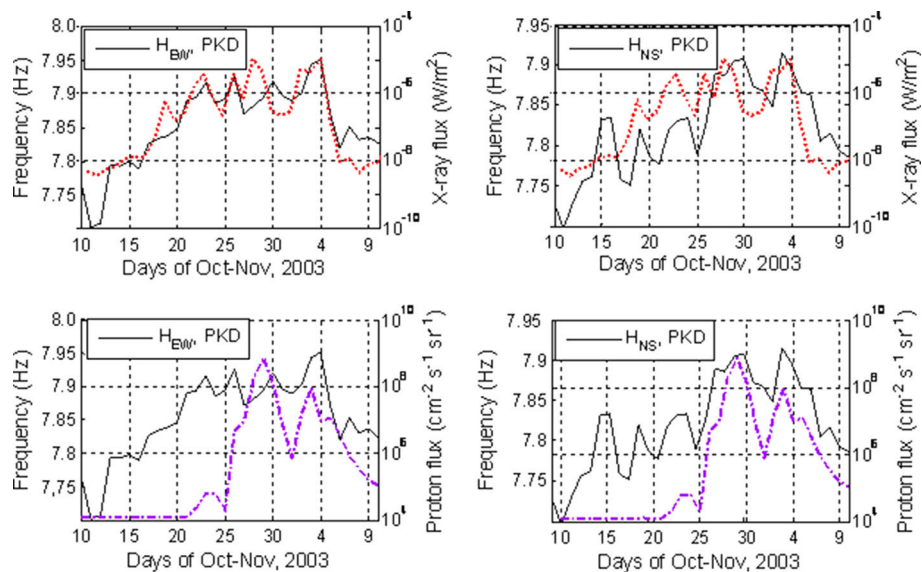


Fig. 9 Simultaneous records of the Schumann resonance frequency variations (in Hertz) during the Halloween Event (October/November, 2003) for the H_{EW} (left panels) and H_{NS} (right panels) components of magnetic field at Parkfield, CA. Superimposed on the frequency records are the histories of the GOES solar X-radiation flux (0.1–0.8 nm wavelength, top panels, red, dashed) and the GOES solar proton flux (>10 MeV, lower panels, purple, dashed)

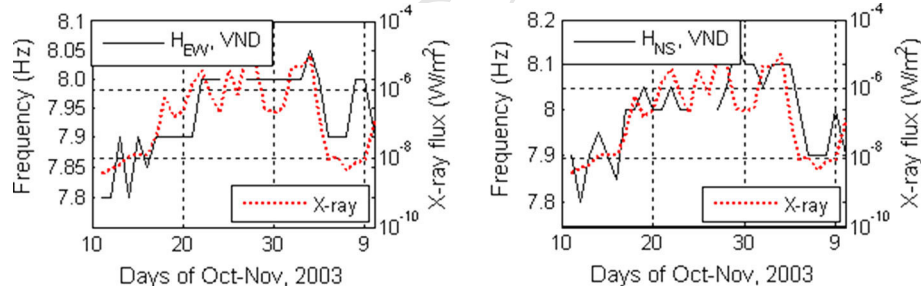


Fig. 10 Simultaneous records of the Schumann resonance frequency variations (in Hertz) during the Halloween event (October/November 2003) for the H_{EW} (left panels) and H_{NS} (right panels) components of magnetic field at Vernadsky, Antarctica. Superimposed on the frequency records are the histories of the GOES solar X-radiation flux (0.1–0.8 nm wavelength, red, dashed, and repeated panel to panel)

342 propagation and shown in Fig. 8. The two effects with the opposite sign of frequency
343 variations canceled each other in the regression analysis. A SO effect might appear in the
344 scatter of frequency values around the regression line due to the day-to-day variability of
345 the global lightning distribution on the timescale of the Halloween event.

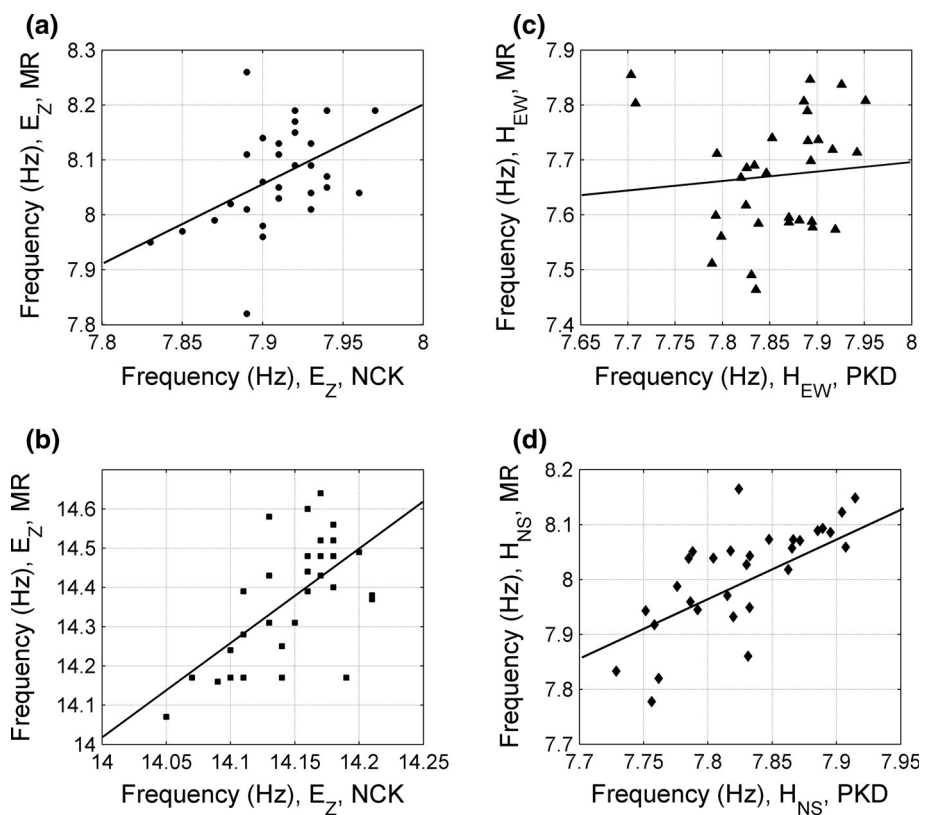


Fig. 11 Regression analysis on simultaneously measured modal frequencies for the different combinations of SR station-pairs **a** NCK–MR, E_Z , 1st mode; **b** NCK–MR; E_Z , 2nd mode; **c** PKD–MR, H_{EW} , 1st mode; **d** PKD–MR, H_{NS} , 1st mode

346 4.2.2 The Halloween Event: Results on Intensity Variations

347 Considerable effort has been invested in looking for an intensity response to the
348 unprecedented X-ray increase in the Halloween event. With the knowledge that the dayside
349 of the Earth is the main recipient of the increased X-ray flux from the Sun, the SR intensity
350 observations at Parkfield were separated into daytime and nighttime contributions. The
351 mean intensities during 10 local daytime hours (8–18 h LT) and 10 local nighttime
352 (20–06 h LT) hours were considered to form two separate time series. Figure 13 shows
353 these two contributions for the full 2-month period (October/November 2003) surrounding
354 the Halloween event. As expected, the daytime intensities are systematically greater than
355 the nighttime ones and additionally a small but discernible increase ($\sim 10\%$) can be noted
356 during the X-ray forcing, especially in the case of the H_{NS} field component (upper right
357 subplot of Fig. 13). It might be considered as the consequence of the changed cavity
358 properties because the H_{NS} field component is responsive for the east–west propagation
359 paths of ELF waves and the cavity in these low-latitude zonal regions can be influenced
360 only by X-ray variations. The problem is that the natural variability of the SR intensity

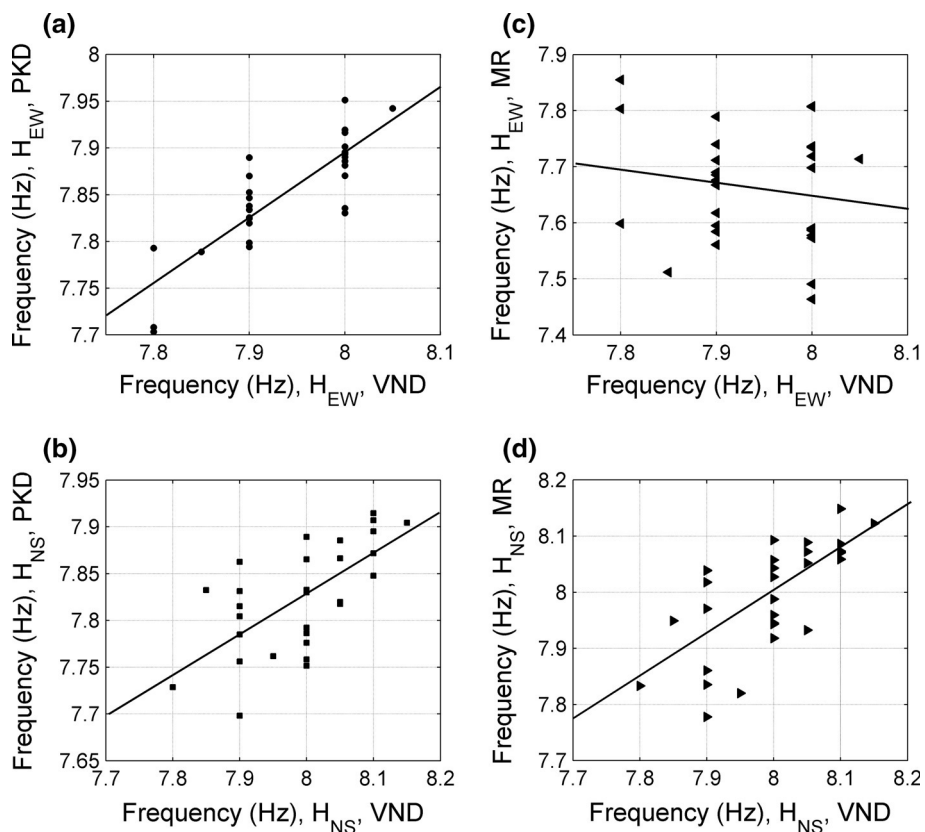


Fig. 12 Regression analysis on simultaneously measured modal frequencies for the different combinations of SR station-pairs **a** VND–PKD, H_{EW} , 1st mode; **b** VND–PKD, H_{NS} , 1st mode; **c** VND–MR, H_{EW} , 1st mode; **d** VND–MR, H_{NS} , 1st mode

361 competes with the predicted changes due to cavity deformation. This point will be further
362 clarified in the interpretation Sect. 5.

363 4.2.3 The Halloween Event: Results on Damping

364 Spectral half-widths given in Hertz (closely related to the reciprocal of the Q factor) were
365 available from the Parkfield station in October–November, 2003. These parameters are
366 characteristic for the damping of the propagating waves in the SR cavity. Figure 14 shows
367 these values for the H_{EW} and H_{NS} field components together with the proton flux variations
368 (upper three subplots) as well as the intensity variation of the E_Z field component available
369 at the Nagycenk Observatory, Hungary (bottom subplot) during October–November days.
370 It can be seen that the damping is slightly increased in the days near the maximum of
371 proton flux and the intensity of E_Z shows a moderate decrease in that time period but the
372 magnitude of the decrease is comparable with the diurnal intensity variations due to
373 changes in the source intensity.

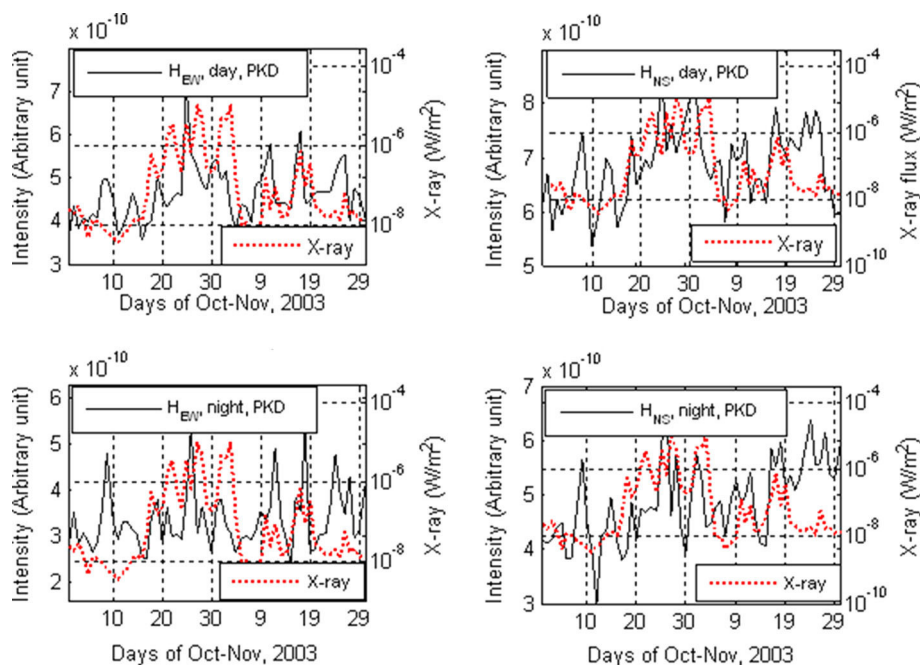


Fig. 13 Simultaneous records of Schumann resonance intensity during the Halloween event (October/November, 2003) at Parkfield, CA for the 2-month interval bracketing the Halloween event. Local daytime records are shown in the top panels and local nighttime records in bottom panels for both components of magnetic fields (H_{EW} left, H_{NS} right). Superimposed on the frequency records are the histories of the GOES solar X-radiation flux (0.1–0.8 nm wavelength, red, dashed, and repeated panel to panel)

374

5 Discussion

375

5.1 Interpretation of Results: Frequencies and Q factors

376

The perturbations to the Earth-ionosphere cavity by ionizing protons and X-radiation are decidedly non-uniform on both short and long timescales, but in keeping with the analytic convenience of earlier work (Sátori et al. 2005), we shall attempt a zeroth-order interpretation of the observations in the context of a uniform cavity. The main observables are Schumann modal frequencies and Q factors. In the context of the uniform knee model (Mushtak and Williams 2002) that is used for the sake of simplicity in the interpretation of observations in this study, the entire cavity response is determined by four physical quantities: two characteristic heights and two conductivity scale heights at the same two altitudes. The approximate nature of this uniform assumption deserves special emphasis in the context of quantitative predictions for the frequency and intensity changes in these energetic solar events. We are confident in the predictions for the *signs* of the frequency changes (consistent with the unanimous agreement among multiple receiving stations within the non-uniform cavity). But no great accuracy is claimed for the magnitudes of the changes, as they are highly dependent on the spectral methods different for nearly all the stations. The use of a more sophisticated day-night model of the cavity and the consistent treatment of time series data from all stations will be needed in future studies toward achieving greater consistency between theory and observation.

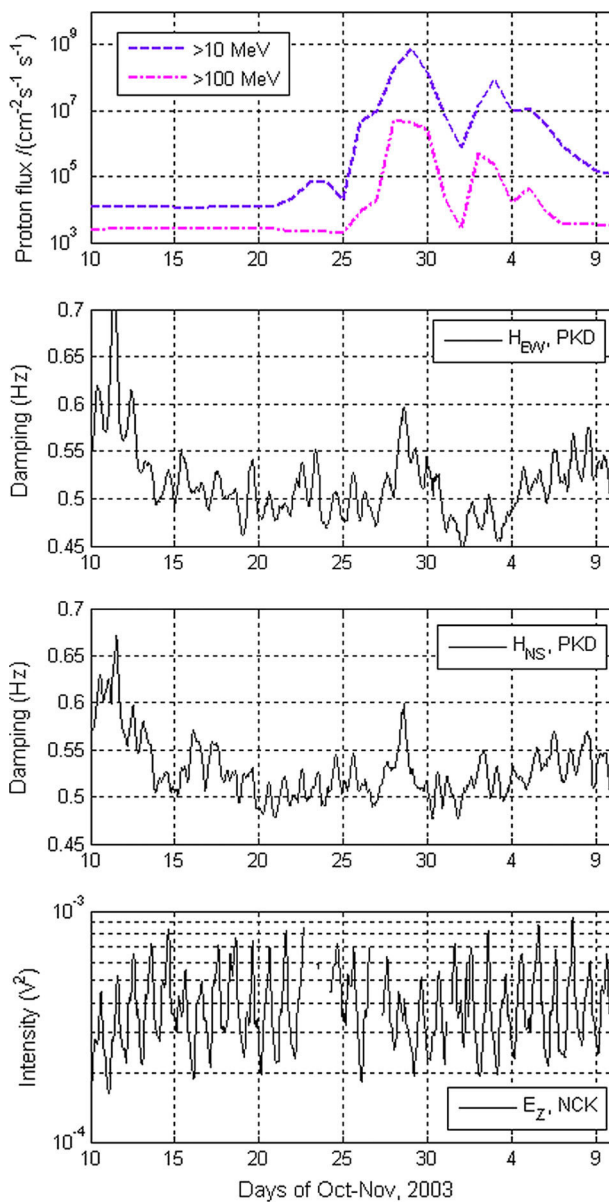


Fig. 14 Simultaneous records of solar proton flux in two energy ranges (top panel) and damping parameter for the H_{EW} (second panel) and H_{NS} (third panel) field component at Parkfield and the SR intensity variation of the E_Z field component (fourth panel) at Nagycenk in October–November days, 2003 of the Halloween event

393
394
395
396

For a fixed Earth circumference, the modal frequencies are physically linked directly with the phase speeds of the waves, and the latter depend on the ratio of the heights. (When the two heights merge at higher frequency (VLF), the phase speed is the speed of light.) Accordingly, the modal frequency is



$$f_n \approx f_n^{(0)} \sqrt{\frac{h_e(f_n)}{h_m(f_n)}}, \quad \text{where} \quad f_n^{(0)} \equiv \left(\frac{c}{2\pi a}\right) \sqrt{n(n+1)} \quad (1)$$

398 The f_n modal frequencies are not exactly the eigenmodal frequencies of the Earth–
400 ionosphere cavity, as they are specified theoretically for a uniform cavity. They are not
401 eigenmodal frequencies due to the overlapping of the neighboring modes in the lossy
402 Earth–ionosphere cavity, and the multiple asymmetries (departures from a uniform cavity)
403 in reality. The observable SR frequencies depend on the cavity properties and on the
404 source–observer distance (Balser and Wagner 1962; Madden and Thompson 1965;
405 Nickolaenko and Hayakawa 2002).

406 Although it is less well known in the SR community, the SR frequencies also depend on
407 the spectral method employed (Verő et al. 2000; Yang and Pasko 2006; Ondráškova and
408 Ševčík 2014). Using the same time series, Verő et al. (2000) compared SR frequencies
409 computed by FFT and complex demodulation, and Yang and Pasko (2006) determined SR
410 frequencies by Lorentzian fitting and Prony algorithm. Both studies found systematic
411 differences (some tenths of Hz) in the frequency values deduced by different spectral
412 techniques. It is important to note that the station-to-station frequency values can be
413 compared quantitatively if they are determined by the same spectral technique.

414 The formula for the global quality factor involves the two heights and in addition, the
415 two scale heights of conductivity at the same two altitudes (Nickolaenko and Rabinowicz
416 1982; Mushtak and Williams 2002). These quantities enter symmetrically in their Q factor
417 dependence.

$$Q_n \equiv \frac{2}{\pi \gamma_n}, \quad \gamma_n \approx \frac{\varsigma_e^{\text{eff}}(f_n)}{h_e(f_n)} + \frac{\varsigma_m^{\text{eff}}(f_n)}{h_m(f_n)} \quad (2)$$

418 The incursions of protons and X-rays lead to reductions in the lower and upper char-
419 acteristic heights, respectively, as discussed in Sect. 3. Reductions in either height alone,
420 with all other quantities remaining constant, lead to reductions in Q factor. In Sátori et al.
421 (2005), the observations showed that for the X-ray response on the solar cycle timescale,
422 both a reduction in upper characteristic height and a reduction in the upper characteristic
423 scale height produced increases in frequency and Q factor consistent with the measured
424 response. In another recent study, Dyrda et al. (2015) document large increases in cavity Q
425 factor associated with a solar flare of short duration. In this study, the separate reduction in
426 lower characteristic height by the energetic proton incursion alone leads to reductions in
427 frequency (shown) and Q factor (not shown) that are broadly consistent with the observed
428 behavior for both the Halloween Day and Bastille Day storms, as well as with earlier
429 observations (and modeling) by Nelson (1967) on solar proton events.

430 The use of Eqs. (1) and (2) for the interpretation of observations is most appropriate
431 when the changes in cavity properties (heights and scale heights) are globally uniform.
432 With the possible exception of the cavity response to changes in galactic cosmic radiation,
433 this uniform scenario is seldom realized. It is well recognized that the bombardment of the
434 Earth’s atmosphere by the X-ray, electron and proton bombardments of the kind consid-
435 ered here is far from globally uniform. The X-radiation comes closest to this idealization,
436 in being quasi-uniform on the sunlit side of the Earth’s atmosphere, though the high-
437 latitude penetration will be diminished on account of the near-grazing incidence.

438 For the Bastille Day event, Table 4 shows that the frequency increase in response to the
439 X-ray event was matched at +0.3 Hz on both magnetic channels. Computations using



Eq. (1), with reference to earlier calculations (Sátori et al. 2005), show that a reduction in the magnetic height h_m from 99 to 92 km, with no change in the electric height h_e would account for the measured change in a uniform waveguide. The observed frequency increase is larger than the one recorded with the same equipment and processing methods at RI in response to the 11-year solar cycle increase in X-radiation documented by Sátori et al. (2005), with a required larger height change by ~ 2 km. Consistent with this larger overall frequency change is the finding that the variation in X-ray intensity for the Bastille Day event exceeded the 100-fold change over the 11-year solar cycle by about 50 %. This is consistent with the larger frequency increase for the Bastille Day event (+0.3 Hz) than for the solar cycle (+0.2 Hz). Regarding the SR response to the following proton flux later in the Bastille Day event (Fig. 2), the largest frequency decrease is recorded in the E_Z field component (Table 4) and is ~ 0.8 Hz. Use of Eq. (1) for a uniform model with the assumption that the proton event involves only a change in h_e shows that a height decrease from 52 to 42 km is required. This diminished height is substantially less than the model prediction (28 km) for the Bastille Day event (Ondráškova 2005), and this may be due to our use of a uniform model for interpretation. The evidence in Fig. 1 suggests that protons with energy in the range of 30–100 MeV dominate this modification in ionospheric height in the magnetically unshielded polar regions, and also validates the assumption that only the lower characteristic height is affected by these protons.

For the Halloween event, we consider again the very consistent frequency response at several stations (Figs. 6, 7, 9, 10) to X-radiation on a substantially longer timescale, supporting the global nature of the response. Table 5 (“Appendix”) shows a frequency increase of ~ 0.2 Hz recorded at Mitzpe Ramon for the fundamental mode. This change is comparable to the first SR response (+0.20 Hz) to the change in X-radiation over the solar cycle in Sátori et al. (2005), but it must be remembered that the competing effects of the protons are superimposed on the X-ray contributions for the Halloween event. In the present case, the use of Eq. (1) for a uniform cavity requires a diminishment of h_m from the reference level (Sátori et al. 2005) of 99 to 94 km to account for the measured frequency change, and with no modification of the lower height h_e .

Regarding the frequency response to the proton arrival that peaks up on October 29 in association with the coronal mass ejection (Lopez et al. 2004) as shown in Fig. 8 or the Halloween event, Table 5 (“Appendix”) shows a frequency decrease of ~ 0.2 Hz in the Hew component of magnetic field. Referring again to Eq. (1) shows that this diminishment of frequency will require a drop in the lower height h_e from the reference level of ~ 52 km (Sátori et al. 2005) to 48 km. This is a rather modest change, and according to the calculations in Fig. 1, which indicates a predominant role of protons with energy not much more than 30 MeV. However, because of the simultaneous occurrence of effects from both protons and X-radiation, serving to dilute the impact of the protons, this interpretation must be treated cautiously.

In pioneering work on this subject, Schlegel and Füllekrug (1999) found increases in daily-averaged Schumann resonance frequencies associated with a collection of nine solar proton events. These observations run counter to both earlier theoretical and experimental results (Madden and Thompson 1965; Nelson 1967), to later observations on the Bastille Day event (Roldugin et al. 2003; De et al. 2010) and other relativistic solar precipitation (Roldugin et al. 1999, 2001), to more recently published results (Zhou and Qiao 2015), and to the results shown in this study for two of the strongest solar proton events on record. Three possible explanations for this apparent discrepancy are suggested. The first is that the events chosen by Schlegel and Füllekrug (1999) involved dominant proton energies not much greater than 1 MeV, and so according to Fig. 1, only the upper characteristic height



of the Schumann cavity is affected, consistent with their own theoretical interpretation. Further resolution here will require a more complete look at the proton energy spectra for the selected events. The second reason is that X-radiation in the same events is not considered. In many proton events, the faster moving X-radiation arrives from the Sun ahead of the protons, and produces systematic frequency increases in SR, on both short (Roldugin et al. 2003, 2004; De et al. 2010; Fig. 2 in this study) and long [Sátori et al. (2005)] timescales, with the general interpretation being that only the upper characteristic layer is affected. This explanation is problematic, however, because in general, after an initial relatively short X-ray event, a much long sustained flux of energetic protons is observed (Roldugin et al. 2004; Belov et al. 2005), which one would expect to dominate the X-ray effects and preferentially influence the lower characteristic height. However, it should also be noted that one of the largest solar proton events (October 1989) documented by Schlegel and Füllekrug (1999) was later shown (Belov et al. 2005) to exhibit an elevated flux of X-radiation throughout the two-week-long event. The third reason is related to the second one. These authors had access to SR frequency changes at the Arrival Heights ELF station with only daily resolution. Given the evidence for variable contributions from different species (X-rays, protons and electrons) at shorter timescales than 1 day may lead to aliasing of the results.

Distinct contrasts in the frequency response on magnetic coils oriented east–west and north–south have been documented for both the Halloween Event (most strongly at the Mitzpe Ramon station, as shown in Fig. 7, and less prominently at Parkfield, as shown in Fig. 9) and for the Bastille Day event (on the Rhode Island station, as shown in Fig. 2). The systematic nature of the observed response, namely a substantially larger lowering of frequency in the EW magnetic field relative to the NS field, was shown earlier for the same Bastille Day event by Nickolaenko and Hayakawa (2002, Fig. 6.30), at another ELF station at Karymshino (53°N , 158°E) in Kamchatka. (In additional documentation of the Bastille Day event by Roldugin et al. (2003), De et al. (2010) and Sanfui et al. (2015), only one SR field component is shown so these contrasts in frequency behavior cannot be explored.) Anisotropic effects on phase speeds of Schumann resonance waves can be expected when the polar regions are more strongly affected by ionizing particles than lower latitudes. In all these cases, reductions in modal frequencies are noted, consistent with a greater separation between the two characteristic heights h_e and h_m in Eq. (1), caused primarily by a lowering of h_e relative to h_m . Charged particles electrons and protons will find easier entry into the lower and upper D-regions of the ionosphere along the Earth's magnetic field lines, where the impact on heights will be more dramatic. Global waves propagating meridionally and sampled in the EW component of magnetic field will propagate through both polar regions, whereas zonally propagating waves, sampled in the NS magnetic field, are expected to be less affected by the polar modifications.

In the same manner that solar proton events induce anisotropy in the frequency response for two magnetic field directions, one might expect that pure X-ray bursts might induce anisotropy by affecting the upper characteristic height at low latitudes preferentially relative to the meridional path linking the polar regions. In this scenario, the Hns frequency is expected to increase more strongly than the Hew frequency. Some slight indication of this expectation can be seen in Fig. 2 for the Rhode Island records for the initial X-ray excursion for the Bastille Day event where one can make comparisons for three resonant modes. A search for such an effect in more numerous but weaker X-ray events in Roldugin et al. (2004) does not show any obvious tendency.



5.2 Interpretation of Results: Intensity Variations

539 The effects of height of the Earth–ionosphere cavity on Schumann resonance intensity
540 have long been recognized (Madden and Thompson 1965; Sentman and Fraser 1991;
541 Schlegel and Füllekrug 1999; Füllekrug et al. 2002; Greifinger et al. 2005). The role of
542 X-radiation and energetic protons in the ionization of D-region altitudes of interest for SR
543 is also well known (Richmond and Venkateswaran 1971; Sentman 1990; Hargreaves 1992;
544 Roldugin et al. 2003, 2004; Ondráškova 2005; Sátori et al. 2005) and has been reviewed in
545 Sect. 3.1. In the context of the analytical treatments for the Earth–ionosphere cavity
546 (Greifinger and Greifinger 1978; Mushtak and Williams 2002; Greifinger et al. 2007), it is
547 essential that the ionizing radiation affect at least one of two characteristic heights to be
548 effective in modifying Schumann resonance intensities. In this context, Williams and
549 Sátori (2007) have emphasized the need for large changes in ionization to enact appre-
550 ciable changes in the two characteristic heights. The reason for this need is that generally
551 height is logarithmic in conductivity, with the implication that an order of magnitude
552 change in conductivity is needed to enact a change in characteristic height (lower or upper)
553 equal to one scale height. One conductivity scale height (~5 km) is typically quite small
554 in comparison with typical characteristic heights (50–90 km).

555 It turns out, however, that for both X-rays and solar proton emission from the Sun, the
556 changes in intensity on record for exceptional events can be several orders of magnitude.
557 Variations in X-ray intensity of two orders of magnitude and more have been documented
558 on both short and long timescales (Belov et al. 2005; Sátori et al. 2005). Documented
559 intensity changes in solar proton events in certain energy ranges can be even more dra-
560 matic. For the Bastille Day event, a five-order-of-magnitude increase of proton flux with
561 energy >100 MeV in hourly time resolution has been documented. For the Halloween
562 event, five- and three-order-of-magnitude increases of energetic proton flux with energies
563 of >10 and >100 MeV, respectively, in daily time resolution were exhibited (<http://spidr.ngdc.noaa.gov/spidr/>). These changes can translate to changes in lower characteristic
564 height amounting to several scale heights.

565 Greifinger et al. (2005) have made predictions based on the transmission line treatment
566 of SR by Kirillov (1996) and others for changes in SR amplitude as a function of changes
567 in ionospheric height.

568 The predictive equations for the field response of the three field components (E_r , H_ϕ and
569 H_θ) to height variations are reproduced below. M_S , which is frequency dependent, is the
570 charge moment of the lightning source, h_e is the lower (capacitive, electric) height and h_m
571 is the upper (inductive, magnetic) height. Parentheticals (S) and (O) refer to heights over
572 the source region and over the observer region, respectively, which were also considered
573 earlier by Madden and Thompson (1965; page 244).

$$E_r(f; S \rightarrow O) \sim M_S(f) \frac{h_m(S)}{h_e(S) h_e(O)} [U(S \rightarrow O)] \quad (3)$$

$$H_\phi(f; S \rightarrow O) \sim M_S(f) \frac{h_m(S)}{h_e(S)} \left[\frac{1}{h_m(O)} \frac{\partial U(S \rightarrow O)}{\partial \theta} \right] \quad (4)$$

$$H_\theta(f; S \rightarrow O) \sim M_S(f) \frac{h_m(S)}{h_e(S)} \left[\frac{1}{h_m(O)} \frac{\partial U(S \rightarrow O)}{\partial \phi} \right] \quad (5)$$



581 The effect of wave propagation between source S and observer O represented by some
582 formula U representing the electric field response to point source excitation along the great
583 circle path between source (S) and observer (O). For a uniform cavity (no lateral variations
584 in heights of either kind) U is analytic, is the voltage on the transmission line represented
585 as the product of the local electric field and the local constant ‘electric’ height, and can be
586 found in works by Wait (1962); Huang et al. (1999), Nickolaenko and Hayakawa (2002)
587 and Sátori et al. (2009). U' is the magnetic field and is obtained analytically from U by
588 application of Faraday’s Law. For the non-uniform cavity, one no longer has an analytical
589 form, and hence the justification for the use of the symbolic forms U and U' above. But
590 despite the loss of the analytic form, the scaling of the fields with waveguide heights is
591 known from the transmission line/telegraph equation analogy. We assume here that during
592 the days of solar events in question, that the distance-dependent variations of U and U' are
593 invariant with time as the source–observer geometries are not appreciably modified from
594 day to day, and so we do not need to know these U , U' quantities in making our predictions
595 for field/intensity changes.

596 Simple assumptions are made here about height variations in X-ray and solar proton
597 events to see what amplitude changes can be expected. As noted earlier, X-rays in the
598 wavelength region 0.1–0.8 nm have a ‘Chapman layer’ in the vicinity of 90 km height
599 (Richmond and Venkateswaran 1971). For the solar X-ray enhancement amounting to two
600 orders of magnitude, and a conductivity increase of about one order of magnitude, the
601 treatment in Sátori et al. (2005) is repeated. This involves a height decrease (at 8 Hz) by
602 about one scale height from $h_m = 99$ km to $h_m' = 94$ km. It should be noted here, how-
603 ever, that the decrease in lower characteristic height consistent with the observed fre-
604 quency change for the uniform model is substantially less than the model prediction (42 vs.
605 28 km). This diluted result is consistent with the realization that the big height change is
606 confined to the polar region, where the protons are guided by the Earth’s magnetic field
607 there where the majority of the Earth’s magnetic field lines enter and exit. Given these
608 estimates for original and perturbed characteristic heights for the two influences of incident
609 X-rays and protons, the equations can be used to estimate percentage changes in field
610 amplitudes. The results of these simple calculations are included in Tables 2 and 3 below,
611 one each for the electric and the magnetic field. Each Table provides estimates for the
612 percentage change in field amplitude for each of two ionization processes (X-rays and
613 protons) and for each of two observer locations (one mid-latitude and one high latitude).
614 Here, we are assuming unperturbed heights $h_e = 52$ km and $h_m = 99$ km, following Sátori
615 et al. (2005) and perturbed heights of $h_e = 42$ km and $h_m = 94$ km. (In this context, it is
616 noteworthy that Ondráškova (2005) estimated a decrease in h_e to 28 km in modeling work
617 on the Bastille Day event.) The impact on h_e at low latitudes is ignored because of
618 magnetic shielding of the protons by the geomagnetic field.

619 In the case of predictions for X-ray effects, the same percentage variations of $h_m(S)$ and
620 $h_m(O)$ can cancel the X-ray effect in the amplitude of the field components. The amplitude
621 decreases (−5 %) if only $h_m(S)$ decreases and the amplitude increases (+5 %) if only
622 $h_m(O)$ decreases. (The intensity changes in percent will be approximately twice these
623 values, namely if the relative amplitude variation is 1 → 1.05 then the relative intensity
624 variation is $1^2 \rightarrow 1.05^2 = 1.1025$, that is ∼10 %.) In general both $h_m(S)$ and $h_m(O)$ vary
625 simultaneously, but with different magnitudes. The symbolic equations enable us to make
626 estimates for a non-uniform cavity, too, in the case of solar X-radiation if the source
627 (S) and the observer (O) are on the different (sunlit or dark) sides of the cavity. Therefore,
628 in Table 2 and 3 for the X-ray variations, a maximum percentage range of (−5 %)–(0 %)
629 is given for SR electric field as well as (−5 %)–(+5 %) for SR magnetic field at 8 Hz.



Table 2 Predicted amplitude changes for Schumann resonance electric field (at 8 Hz), based on the symbolic Eq. (3)

	Mid-latitude observer	High-latitude observer
X-radiation	(−5 %)–(0 %)	(−5 %)–(0 %)
Proton	0 %	+19 %

The global lightning source is assumed to predominate at low latitude

Table 3 Predicted amplitude changes for Schumann resonance magnetic field (at 8 Hz), based on the symbolic Eqs. (4) and (5)

	Mid-latitude observer	High-latitude observer
X-radiation	(−5 %)–(+5 %)	(−5 %)–(+5 %)
Proton	0 %	+11 %

The global lightning source is assumed to predominate at low latitude

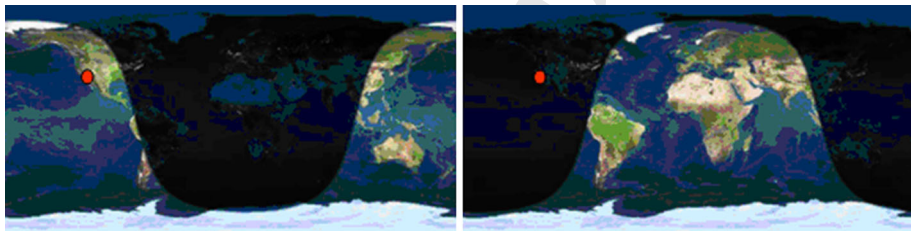


Fig. 15 Sunlit and dark side of the Earth when the Parkfield SR station (indicated with red dot) is on the dayside at 15 h LT (left) and on the nightside at 03 h LT (right)

630 Parkfield is in a special geographical position as shown in Fig. 15. There are several local
631 daytime hours when the main tropical chimney regions are mostly under nighttime con-
632 ditions during the Halloween event, and the X-ray effect on $h_m(S)$ can be neglected while
633 $h_m(O)$ decreases. This can explain why the magnetic field intensity increases at Parkfield in
634 local daytime hours during the days of the Halloween event (see Fig. 13). With the
635 exception of the high-latitude observer, for which localized effects on amplitude are
636 dominant, the predicted changes in amplitude for low-to-mid-latitude stations are quite
637 modest at only a few percent. At high latitude, the expectation for a large positive
638 amplitude effect is dependent on a decrease in h_e over the observer for the electric field
639 prediction. It means ~19 % increase of E_Z amplitude if $h_e(O)$ changes from 52 to 42 km.
640 It can also be supposed that protons with smaller energies (<3 MeV, see Fig. 1) can
641 influence $h_m(O)$, too, and consequently the magnetic field components can also increase.
642 For example if $h_m(O)$ changes from 99 to 88 km, this means an ~11 % increase in the
643 magnetic amplitudes. It can be stated that the increase of the field amplitudes in the polar
644 region is highly dependent on the energy of the incoming protons (charged particles).

645 A search for SR intensity changes at mid-latitude station associated with the Bastille
646 Day event (Figs. 3 and 4) West Greenwich, Rhode Island, was shown earlier in Sect. 4, no



647 conspicuous evidence was found and a ~10 % intensity increase related to the bursty
648 X-ray period of the Halloween event was identified in the magnetic field component at
649 Parkfield, but only in the daytime hours and mainly for the H_{NS} field component (see
650 Fig. 13). An intensity decrease of some ten percent appeared in the vertical electric field
651 component at Nagycenk (see Fig. 14) during the quasi-simultaneous episodes of the
652 energetic proton flux and the main depression of the huge Forbush-decrease. The latter
653 event can result in an increase of the $h_e(O)$ and consequently an additional decrease of E_Z
654 due to the decreased cosmic ray ionization with the Forbush-decrease (the first equation in
655 the set of three above). However, the increased damping corresponds to an expected
656 decrease of the Q factor at PKD, contrary to the predictions based on the analytical
657 expression for Q factor. So the uniform model seems inadequate to describe this com-
658 plicated condition. We did not make model predictions for the damping parameter for the
659 results shown in Fig. 14.

660 These results are consistent with the predictions for amplitude changes in Tables 2 and
661 3 for the electric and magnetic field, together with the competition from the natural
662 variability of the intensity which amounts to tens of percent on these relatively short
663 timescales.

664 These findings are also consistent with a host of earlier published results at mid-latitude
665 stations. For example, Sentman (1996) found no measureable response in SR intensity to
666 large solar storms in the fall of 1989 [the same storms also investigated by Schlegel and
667 Füllekrug (1999) at a high-latitude site] at two mid-latitude stations in California and
668 Australia. Likewise, Roldugin et al. (1999) found no substantial response of the SR
669 amplitude to solar proton events. Roldugin et al. (2001) reported a mixture of results for
670 four solar events in the 1997–1998 time frame. In two cases, decreases of the order of tens
671 of percent in magnetic amplitude were noted, in a third a weak decrease of amplitude and
672 in the fourth no change was detected. The negative signs of the observed changes are also
673 possible in accordance with the predictions in Table 3 but the magnitudes are on the high
674 side, and questions remain about the reality of the physical linkages, given the natural
675 variability. In a still later analysis pertaining to the Bastille Day event, Roldugin et al.
676 (2004) reported: “Neither in Lovozero (68°N, 35°E) nor in Karymshino (53°N, 158°E) any
677 appreciable effect (in magnetic amplitude) is found in any components and modes.”

678 Regarding the situation at high latitude, it is important to note the predictions for
679 magnetic amplitude for the observer at high latitude where the height change is local to that
680 location (the second equation in the set of three above). The magnetic amplitude change is
681 appreciable only if the upper characteristic height h_m is reduced, as noted above. This
682 prediction is consistent with the inconspicuous change in the Vernadsky magnetic intensity
683 at the time of the large proton flux for the Halloween event. For solar protons, we now have
684 abundant evidence that it is the lower height that is affected, not the upper one. The
685 remaining puzzle pertains to the daily mean amplitude increases up to a few tens of percent
686 at Arrival Heights, another high-latitude station, reported by Schlegel and Füllekrug
687 (1999). This would suggest that the h_m values are reduced in keeping with their theoretical
688 interpretation, but not in keeping with the evidence that energetic protons are more likely
689 to lower the h_e values.

690 5.3 Similarities on the Longer Timescale of the 11-year Solar Cycle

691 Part of the motivation for investigating the effects of energetic solar emissions on short
692 timescales came from the earlier analysis on the 11-year solar cycle timescale (Sátori et al.
693 2005). In that work, it was shown that a two-order-of-magnitude increase in hard X-radiation

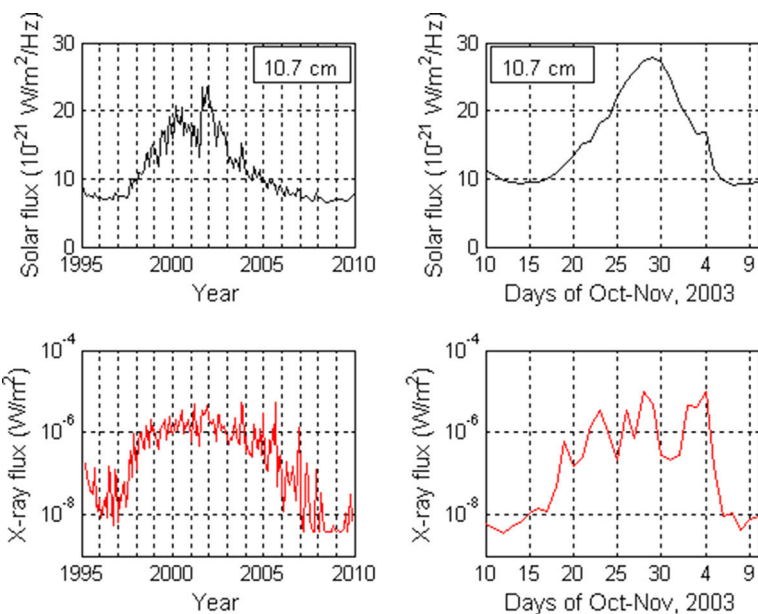


Fig. 16 Flux comparisons on long (11-year solar cycle, *left panel*) and short (\sim 2-week period of ‘Halloween’ event in October/November, 2003, *right panel*). *Upper plots* represent 10.7 cm radiation flux. *Lower plots* show GOES solar X-radiation (0.1–0.8 nm wavelength) fluxes. The variations in both fluxes are of comparable magnitude on these two quite different timescales

at solar maximum was responsible for a worldwide increase in Schumann resonance modal frequencies. Now that the Halloween event has been explored on a timescale intermediate between the single-day Bastille Event and the 11-year solar cycle, we are now equipped to address the evidence for a timescale independence of the SR X-ray response. Figure 16 compares records of 10.7 cm radiation and sustained X-radiation from the Sun for the 11-year solar cycle on the left and the Halloween event on the right. The 10.7 cm solar radiation is generally used as an indication of solar EUV radiation which is the main ionization source of the upper D-region in daytime. In this depiction, the time history of the Halloween event appears as a miniature version of the solar cycle, though with slightly elevated radiation levels in comparison with the solar cycle. The SR frequency variations follow most closely the time history of the bursty period of X-radiation of more than two orders of magnitude of flux changes as shown in Figs. 6, 7, 9 and 10. The frequency variations do not run parallel with the \sim threefold flux changes in the 10.7 cm solar radiation (Williams and Sátori 2007). The systematic and conspicuous positive SR frequency response to X-radiation during the Halloween event has been documented in Figs. 6, 7, 9 and 10 and a similar response to X-radiation on much shorter timescale in the Bastille Day event in Fig. 2. Yet another short term X-ray event was documented in Sátori et al. (2005). Now the SR responses can be assembled for comparison in Tables 4, 5, 6, 7 and 8 in the “Appendix”. The sign of the frequency variations can be compared and the magnitudes, too, if the frequencies were determined by the same spectral technique like as at RI and in MR. Here, it is seen that the frequency increases for the 1st SR mode are ordered by the magnitude of the X-radiation flux, independent of the timescale over which the event occurs.

When the records of energetic protons are considered on the widely different timescales of the Halloween event and the 11-year solar cycle, less similarity is apparent. The duty



cycle of the protons for the Halloween event is substantially larger than for the solar cycle, with more than half of the overall period of enhanced X-radiation also exhibiting proton enhancements (Fig. 5). On the latter timescale, the general incidence of energetic protons follow the solar cycle and with a rough two-order-of-magnitude change, but the proton flux is highly episodic (Feynman et al. 1990) by comparison and in marked contrast with the quasi-steady variation in the background X-radiation (Veronig et al. 2004) also shown in Fig. 16. The search for an explanation of the sustained enhancement of SR magnetic intensity near solar maximum at the high-latitude station at Vernadsky (Antarctica) arose in this context (Williams et al. 2014). It was also noticed that independent estimates of ionospheric height on a global basis showed a noticeable reduction sustained in time at higher latitude (Toledo-Redondo et al. 2012). The impact of local height changes on SR amplitude was first noted by Madden and Thompson (1965, page 244) but that has since been quantified (Greifinger et al. 2005) with the Eqs. (3) to (5) by the local observer height. A key point in the interpretation of Eq. (4) is that no appreciable increase in amplitude will be manifest at the high-latitude station unless the upper (magnetic) magnetic height is lowered. Yet much evidence has accrued in this study that protons will affect primarily the lower characteristic height there, and indeed, little change in magnetic intensity was noted at Vernadsky (not shown) in response to the energetic protons in the Halloween event. But returning to the solar cycle timescale, if 50 keV electrons are available, Fig. 1 shows that they are most likely to affect the upper characteristic height and on the basis of Eqs. (4) and (5) lead to an enhanced amplitude at solar maximum. Recent discussions (D. Baker, B. Blake and H. Spence, personal communication, December 2014) indicate that such energetic electrons are available from the Earth's inner radiation belt and may be the main players in modulating the SR intensity at Vernadsky over the 11-year solar cycle. This suggestion is currently under further investigation.

6 Conclusions

The main conclusions to be drawn from this work are as follows:

1. Generally speaking, X-rays with wavelengths in the 0.1–0.8 nm range affect the upper characteristic height and solar protons primarily the lower characteristic height of the SR cavity. This result is already well known but is strongly substantiated by results shown here, and the unanimous multiple-station documentation assures the global nature of the phenomena. The linkage with specific altitudes of the ionosphere is consistent with independently published results on penetration depth versus particle energy.
2. Time-resolved frequency variations are essential in diagnosing independent ionizing effects of X-rays and energetic protons on the Earth–ionosphere cavity.
3. The effect of X-radiation on SR frequency increase is not monotonic with X-ray flux and this is probably due to the overlapping effects of the protons that typically force the phase speeds of ELF waves and the attendant modal frequencies in the opposite direction.
4. The impact of charged particle events, most notably the energetic proton events on short timescales, is predominant in polar regions. As a consequence, ELF propagation paths in the meridional direction are more strongly affected than those in the zonal direction. The larger frequency decreases in the east–west magnetic field components compared to the north–south components is consistent with this physical picture.
5. In response to solar events, the SR response in frequency is most conspicuous and in amplitude least conspicuous (consistent with earlier work by Williams and Sátori 2007).



763 6. The inconspicuous response of SR amplitude/intensity to the most energetic solar
 764 events on record is consistent with theoretical considerations and provides additional
 765 indirect evidence that the SR intensity is primarily a record of the lightning activity
 766 within the Earth-ionosphere cavity. This finding provides additional encouragement to
 767 make use of the natural framework of SR to monitor the global lightning activity in
 768 absolute units (Williams and Mareev 2014).

769 Future analyses of major perturbations of the SR will benefit from the use of a cavity
 770 model with both day–night and polar asymmetry, and a common processing of all receiver
 771 data sets for the same modal frequencies.

772 **Acknowledgments** Discussions with Dan Baker, Anatoly Belov, Bern Blake, Steve Cummer, Barbara
 773 Emery, Martin Füllekrug, István Lemerger, Adriena Ondráškova, Steve Park, Craig Rodger, Valentin
 774 Roldugin, Harlan Spence and Rob Steenburgh are greatly appreciated. Alexander Melnikov provided major
 775 assistance with the organization of the Parkfield and Mitzpe Ramon data in early stages. The authors are
 776 thankful to the National Antarctic Scientific Center of Ukraine, Ministry of Education and Science of
 777 Ukraine for providing the ELF data recorded at the Ukrainian Antarctic Station “Academic Vernadsky”.
 778 The contribution of Earle Williams to this study was funded by the Hungarian Academy of Sciences as part
 779 of a Visiting Fellowship to the Research Centre for Astronomy and Earth Sciences, Geodetic and Geo-
 780 physical Institute in Sopron. The contribution of Gabriella Sátori was supported by the National Research,
 781 Development and Innovation Office, Hungary—NKFIH, K115836.
 782

783 Appendix

784 Tables of Modal Frequency Variations in Response to Specific Solar Events

785 See Tables 4, 5, 6, 7 and 8.

786

787

Table 4 Schumann resonance modal frequency changes at West Greenwich, Rhode Island, for the Bastille Day event: July 14, 2000

Mode number	RI, E_Z		RI, H_{EW}		RI, H_{NS}	
	X-ray burst (Hz)	Proton flare (Hz)	X-ray burst (Hz)	Proton flare (Hz)	X-ray burst (Hz)	Proton flare (Hz)
1st mode	+0.2	-0.8	+0.3	-0.5	+0.3	-0.3
2nd mode	+0.3	-1.0	+0.5	-1.0	+0.5	-1.0
3rd mode	+0.5	-1.2	+0.5	-1.0	+0.7	-1.2

Table 5 Schumann resonance modal frequency changes at Mitzpe Ramon, Israel, for the Halloween Event: October–November, 2003

Mode number	MR, E_Z		MR, H_{EW}		MR, H_{NS}
	X-ray (Hz)	X-ray (Hz)	X-ray (Hz)	Proton flare (Hz)	X-ray (Hz)
1st mode	+0.2	+0.2z	+0.2z	-0.2	+0.2
2nd mode	+0.3	+0.6	+0.6	-0.6	+0.4
3rd mode	+0.4	+0.5	+0.5	-0.5	+0.5



Table 6 First mode Schumann resonance frequency changes at Parkfield, California, for the Halloween Event: October–November, 2003

Mode number	PKD, H_{EW} X-ray (Hz)	PKD, H_{NS} X-ray (Hz)
1st mode	+0.1	+0.1

Table 7 First mode Schumann resonance frequency changes at Vernadsky, Antarctica, for the Halloween Event: October–November, 2003

Mode number	VND, H_{EW} X-ray (Hz)	VND, H_{NS} X-ray (Hz)
1st mode	+0.1	+0.1

Table 8 Schumann resonance modal frequency changes at Nagycenk Observatory (Hungary) for the Halloween Event: October–November, 2003

Mode number	NCK, E_Z X-ray (Hz)
1st mode	+0.1
2nd mode	+0.1

788

References

- 789 Baker DN, Kanekal SG, Li X, Monk SP, Goldstein J, Burch JL (2004) An extreme distortion of the Van
790 Allen belt arising from the Halloween solar storm in 2003. *Nature* 432:878–881
791 Balser M, Wagner C (1962) On frequency variations of the Earth–ionosphere cavity modes. *J Geophys Res*
792 67:4081–4083
793 Belov A, Garcia H, Kurt V, Mavromichalaki E (2005) Proton events and X-ray flares in the last three solar
794 cycles. *Cosm Res* 43:165–178
795 Bieber JW, Dröge W, Evenson PA, Pyle R (2002) Energetic particle observations during the 2000 July 14
796 solar event. *Astrophys J* 567:622–634
797 Brasseur G, Solomon S (1986) Aeronomy of the middle atmosphere, Second Edition edn. D. Reidel Pub-
798 lishing Company, Dordrecht/Boston/Lancaster
799 Chapman FW, Jones DL (1964) Earth–ionosphere cavity resonances and the propagation of extremely low
800 frequency radio waves. *Nature* 177:930–933
801 De SS, De BK, Bandyopadhyay B, Paul S, Haldar DK, Barui S (2010) Studies on the shift in the frequency
802 of the first Schumann resonance mode during a solar proton event. *Atmos Res* 72:829–836
803 Dyrda M, Kulak A, Mlynarczyk J, Ostrowski M (2015) Novel analysis of a sudden ionospheric disturbance
804 using Schumann resonance measurements. *J Geophys Res Space Phys* 120:2255–2262. doi:[10.1002/2014JA020854](https://doi.org/10.1002/2014JA020854)
805 Feynman J, Armstrong TP, Dao-Gibner L, Silverman S (1990) New interplanetary proton fluence model.
806 *J Spacecr* 27:403–410
807 Füllekrug M (1994) Schumann-Resonanzen in den Magnetfeld-Komponenten, Doctoral dissertation,
808 University of Göttingen, Germany
809 Füllekrug M, Fraser-Smith AC, Schlegel K (2002) Global ionospheric D-layer height monitoring. *Europophys*
810 *Lett* 59:626–629
811



- 812 Getselev V, Okhlopkov VP, Podzolko MV (2006) Solar cosmic ray proton fluxes in the Earth's orbit. In:
813 Physics of auroral phenomena, proceedings of the XXIX annual seminar, apatity. Kola Science Centre,
814 Russian Academy of Science, pp 179–182
- 815 Greifinger C, Greifinger P (1978) Approximate method for determining ELF eigenvalues in the Earth–
816 ionosphere waveguide. *Radio Sci* 13:831–837
- 817 Greifinger P, Mushtak V, Williams E (2005) The lower characteristic ELF altitude of the Earth–ionosphere
818 waveguide: Schumann resonance observations and aeronomical estimates. In: 6th international sym-
819 posium on electromagnetic compatibility and electromagnetic ecology, St. Petersburg State Elec-
820 trotechnical University
- 821 Greifinger PS, Mushtak VC, Williams ER (2007) On modeling the lower characteristic ELF altitude from
822 aeronomical data. *Radio Sci* 42:RS2S12. doi:10.1029/2006RS003500
- 823 Hargraves JK (1992) The solar-terrestrial environment. Cambridge University Press, Cambridge
- 824 Kirillov VV (1996) Two-dimensional theory of ELF electromagnetic wave propagation in the Earth–
825 ionosphere waveguide channel. *Radiophys Quantum Electron* 39:737–743
- 826 Kulak A, Mlynarczyk J (2013) ELF propagation parameters for the ground-ionosphere waveguide with finite
827 ground conductivity. *IEEE Trans Antennas Propag* 61:2269–2275
- 828 Kulak A, Kubisz J, Michalec A, Ziba S, Nieckarz Z (2003) Solar variation in extremely low propagation
829 parameters: 2. Observations of Schumann resonances and computation of the ELF attenuation
830 parameter. *J Geophys Res* 108(A7):1271
- 831 **AQ5** Kulak A, Mlynarczyk J, Zieba S, Micek S, Niecharz Z (2006) Studies of ELF propagation in the spherical
832 shell cavity using a field decomposition method based on asymmetry of Schumann
833 Le G, Han Y, Zhang Y (2007) A comparative analysis of two solar proton events. *Chin Sci Bull* 52:47–51
- 834 Lopez RE, Baker DN, Allen J (2004) Sun unleashes Halloween storm. *EOS* 85:105–108
- 835 Madden T, Thompson W (1965) Low-frequency electromagnetic oscillations of the Earth–ionosphere
836 cavity. *Rev Geophys* 3:211–254
- 837 Mushtak VC, Williams ER (2002) ELF propagation parameters for uniform models of the Earth–ionosphere
838 waveguide. *J Atmos Sol Terr Phys* 64:1989–2001
- 839 Nelson PH (1967) Ionospheric perturbations and Schumann resonance data. Project NR-371-401, Geo-
840 physics Laboratory, Massachusetts Institute of Technology, Cambridge, MA
- 841 Nickolaenko AP (1997) Modern aspects of Schumann resonance studies. *J Atmos Terr Phys* 59:805–816
- 842 Nickolaenko AP, Hayakawa M (2002) Resonances in the Earth–ionosphere cavity. Kluwer Academic
843 Publisher, Dordrecht, London
- 844 Nickolaenko AP, Hayakawa M (2014) Schumann resonance for tyros: essentials of global electromagnetic
845 resonance in the Earth–ionosphere cavity. Springer, Tokyo/Heidelberg/New York/Dordrecht/London
- 846 Nickolaenko AP, Rabinowicz LM (1982) Possible global electromagnetic resonances on the planets of Solar
847 system. *Space Res* XX(1):82–88, 1982 (Trans Kosmicheskie Issledovaniya 20(1):82–88, Jan–Feb
848 Nickolaenko AP, Kudintseva IG, Pechony O, Hayakawa M, Hobara Y, Tanaka YT (2012) The effect of a
849 gamma ray flare on Schumann resonances. *Ann Geophys* 30:1321–1329
- 850 Ondráškova A (2005) The D-region ion composition and electron density response to strong solar proton
851 events (model simulations). *Adv Space Res* 35:440–444
- 852 Ondráškova A, Ševčík S (2014) The determination of Schumann resonance mode frequencies using iterative
853 procedure of complex demodulation. *Contrib Geophys Geodesy* 44(4):313–328
- 854 Ondráškova A, Krivolutsky A, Laštovička J (2003) Changes of the neutral and ionized composition in the
855 D-region after solar proton event in October 1989 (model simulations). *Adv Space Res* 31:2169–2176
- 856 Ondráškova A, Ševčík S, Kostecký P (2011) Decrease of Schumann resonance frequencies and changes in
857 the effective lightning areas toward the solar cycle minimum of 2008–2009. *J Atmos Solar Terr Phys*
858 73:534–543
- 859 Palmer DM et al (2005) Gamma ray observations of a giant flare from the Magnetar SGR 1806–20. *Nature*
860 434(1):107–1109
- 861 Price C, Mushtak V (2001) The impact of the August 27, 1998, γ -ray burst on Schumann resonances.
862 *J Atmos Sol Terr Phys* 63:1043–1047
- 863 Rabinowicz LM, Shvets AV, Nickolaenko AP (2008) Polar non-uniformity of ionosphere related to solar
864 proton events. *Telecommun Radio Eng* 67(5):413–435
- 865 Rees MH (1989) Physics and chemistry of the upper atmosphere, 1st edn. Cambridge University Press,
866 Cambridge
- 867 **AQ6** Reid GC (1986) Solar energetic particles and their effects on the terrestrial environment. In: The physics of
868 the sun. Elsevier
- 868 **AQ7** Richardson JD, Wang C, Paularina KI (2001) The solar wind: from solar minimum to maximum. *Adv Space
870 Res* 27:471–479



- 871 Richmond AD, Venkateswaran SV (1971) Geomagnetic crochets and associated ionosphere current systems.
872 Radio Sci 6:139–164
- 873 Roldugin VC, Maltsev YP, Vasiljev AN, Vashenyuk EV (1999) Changes of the first resonance frequency
874 during relativistic solar proton precipitation in the 6 November 1997 event. Ann Geophys
875 17:1293–1297
- 876 Roldugin VC, Maltsev YP, Petrova GA, Vasiljev AN (2001) Decrease of the first Schumann resonance
877 frequency during solar proton events. J Geophys Res 106:18555–18562
- 878 Roldugin VC, Maltsev YP, Vasiljev AN, Shvets AV, Nickolaenko AP (2003) Changes of Schumann
879 resonance parameters during the solar proton event of July 14, 2000. J Geophys Res 108(A3):1103
- 880 Roldugin VC, Maltsev YP, Vasiljev AN, Schokotov AY, Belyajev GG (2004) Schumann resonance fre-
881 quency increase during solar X-ray bursts. J Geophys Res 109:A01216. doi:[10.1029/2003JA010019](https://doi.org/10.1029/2003JA010019)
- 882 [AQS] Sanfui M, Haldar DK, Biswas D (2015) Studies on different geophysical and extra-terrestrial events within
883 the Earth–ionosphere Cavity in terms of ULF/ELF/VLF radio waves. *Astrophys Space Sci* (in final
884 review)
- 885 Sátori G, Szendrői J, Verő J (1996) Monitoring Schumann resonances-I. Methodol J Atmos Terr Phys
886 58:1475–1481
- 887 Sátori G, Williams ER, Boldi R, Füllekrug M (2000) Systematic variations of Schumann resonances
888 frequencies on the 11-year solar cycle at multiple stations. EOS Trans AGU 81(48):A12B-01
- 889 Sátori G, Williams E, Mushtak V (2005) Response of the Earth–ionosphere cavity resonator to the 11-year
890 solar cycle in X-radiation. J Atmos Sol Terr Res 67:553–562
- 891 [AQ9] Sátori G, Mushtak V, Williams E (2009) Schumann resonance signature of global lightning activity. In: Betz
892 HD, Schumann U, Laroche P (eds) Lightning: principles, instruments and applications: review of
893 modern lightning research. Springer, Berlin, pp 347–386
- 894 Schlegel K, Füllekrug M (1999) Schumann resonance parameter changes during high-energy particle pre-
895 precipitation. J Geophys Res 104:10111–10118
- 896 Schumann WO (1952) Über die strahlungsgesetzen Eigenschwingungen einer leitenden Kugel, die von einer
897 Luftsicht und einer Ionosphärenhülle umgeben ist. Z Naturforsch A 7:6627–6628
- 898 Sentman DD (1990) Approximate Schumann resonance parameters for a two-scale-height ionosphere.
899 J Atmos Terr Phys 52:35–46
- 900 Sentman, DD, Heavner MJ, Baker DN, Cayton TE, Fraser BJ (1996) Effects of solar storms on the
901 Schumann resonances in late 1989. In: 10th Annual conference on atmospheric electricity, society of
902 atmospheric electricity of Japan
- 903 Sentman DD, Fraser BJ (1991) Simultaneous observations of Schumann resonances in California and
904 Australia: evidence for intensity modulation of the local height of the D-region. J Geophys Res
905 96:15973
- 906 Shvets AV, Nickolaenko AP, Belyaev GG, Schekotov AY (2005) Analysis of Schumann resonance
907 parameter variations associated with solar proton events. Telecommun Radio Eng 64(9):771–791
- 908 Tanaka YT, Hayakawa M, Hobara Y, Nickolaenko AP, Yamashita K, Sato M, Takahashi Y, Terasawa T,
909 Takahashi T (2011) Detection of transient ELF emission caused by the extremely intense cosmic
910 gamma-ray flare of 27, December 2004. Geophys Res Lett 38:L08805. doi:[10.1029/2011GL047008](https://doi.org/10.1029/2011GL047008)
- 911 Thomson NR, Rodger CJ, Dowden RL (2004) Ionosphere gives size of greatest solar flare. Geophys Res Lett
912 31:L06803. doi:[10.1029/2003GL019345](https://doi.org/10.1029/2003GL019345)
- 913 Toledo-Redondo S, Parrot M, Salinas A (2012) Variation of the first cut-off frequency of the Earth–
914 ionosphere waveguide observed by DEMETER. J Geophys Res 117:A04321. doi:[10.1029/2011JA017400](https://doi.org/10.1029/2011JA017400)
- 915 Verő J, Szendrői J, Sátori G, Zieger B (2000) On spectral methods in Schumann resonance data processing.
916 Acta Geod Geophys Hungaria 35:105–132
- 917 Veronig AM, Temmer M, Hanslmeier A (2004) The solar soft X-ray background flux and its relation to flare
918 occurrence. Sol Phys 219:125–133
- 919 Wait JR (1962) Electromagnetic waves in stratified media. Pergamon, New York
- 920 Whitten RC, Popoff IG (1971) Fundamentals of aeronomy. Wiley, New York
- 921 Williams ER, Mareev EA (2014) Recent progress on the global electrical circuit. Atmos Res
922 135–136:208–227
- 923 Williams ER, Sátori G (2007) Solar radiation-induced changes in ionospheric height and the Schumann
924 resonance waveguide on different timescales. Radio Sci. doi:[10.1029/2006RS003494](https://doi.org/10.1029/2006RS003494)
- 925 Williams E, Guha A, Boldi R, Sátori G, Koloskov A and Yampolski Y (2014) Global circuit response to the
926 11-year solar cycle: changes in source or in medium? XV. In: International conference on atmospheric
927 electricity, Norman, Oklahoma
- 928



- 929 Yang H, Pasko VP (2006) Three-dimensional finite difference time domain modeling of the diurnal and
930 seasonal variations in Schumann resonance parameters. *Radio Sci* 41:RS2S14. doi:[10.1029/2005RS003402](https://doi.org/10.1029/2005RS003402)
- 931 Zhou H, Qiao X (2015) Studies on the variations of the first Schumann resonance frequency during the solar
932 X-ray burst on 7 March 2012. *J Geophys Res (Atmospheres)*. doi:[10.1002/2014JD022696](https://doi.org/10.1002/2014JD022696)
- 933